City of Morro Bay and
Cayucos Sanitary District

OFFSHORE MONITORING AND REPORTING PROGRAM

QUARTERLY REPORT

WATER-COLUMN SAMPLING APRIL 2007 SURVEY

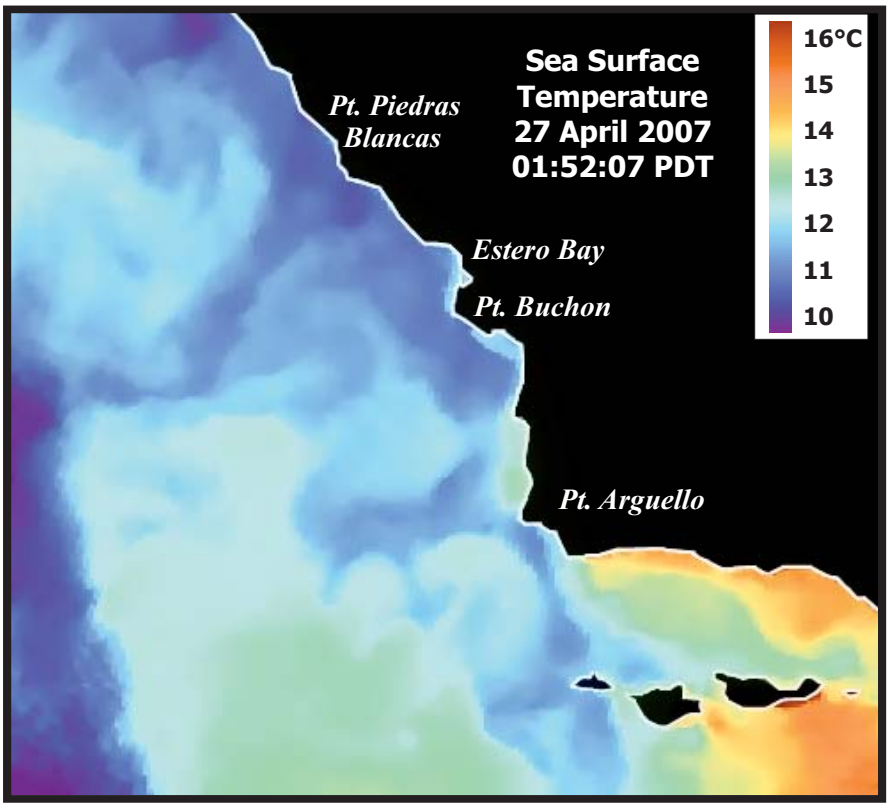

Marine Research Specialists

3140 Telegraph Rd., Suite A
Ventura, California 93003

Report to

City of Morro Bay and
Cayucos Sanitary District

955 Shasta Avenue
Morro Bay, California 93442
(805) 772-6272

OFFSHORE MONITORING AND REPORTING PROGRAM

QUARTERLY REPORT

WATER-COLUMN SAMPLING APRIL 2007

Prepared by

Douglas A. Coats
and
Bonnie Luke

Marine Research Specialists

3140 Telegraph Rd., Suite A
Ventura, California 93003

Telephone: (805) 644-1180
Telefax: (805) 289-3935
E-mail: Doug.Coats@mrsenv.com

May 2007

marine research specialists
3140 Telegraph Road, Suite A · Ventura, CA 93003 · (805) 644-1180

Mr. Bruce Keogh
Wastewater Division Manager
City of Morro Bay
955 Shasta Avenue
Morro Bay, CA 93442

24 May 2007

Reference: Quarterly Receiving-Water Report – April 2007

Dear Mr. Keogh:

Enclosed is the Quarterly Report for the Water-Quality Survey conducted on Saturday, 28 April 2007. This second-quarter survey assessed the effectiveness of effluent dispersion during spring oceanographic conditions. Based on quantitative analyses of continuous instrumental measurements and qualitative visual observations, the wastewater discharge was found to be in compliance with the receiving-water limitations specified in the NPDES discharge permit, and with the objectives of the California Ocean Plan.

High-precision measurements clearly delineated discharge-related perturbations in four of the six seawater properties at two of the sixteen sampling stations. Both stations were located near the boundary of the zone of initial dilution. The anomalies in all of the seawater properties, except salinity, were generated by the upward displacement of ambient seawater entrained within the effluent plume. Dilution levels determined from the salinity anomalies within the discharge plume significantly exceeded those anticipated by modeling and outfall design criteria. Thus, all of the measurements were indicative of low organic loading within the discharged wastewater, and of an outfall operating as designed.

Please contact the undersigned if you have any questions regarding the attached report.

Sincerely,

Douglas A. Coats, Ph.D.
Program Manager

Enclosure (Five Report Copies)

I certify under penalty of law that this document and all attachments were prepared under my direction or supervision in accordance with a system designed to assure that qualified personnel properly gather and evaluate the information submitted. Based on my inquiry of the person or persons who manage the system, or those persons directly responsible for gathering the information, the information submitted is, to the best of my knowledge and belief, true, accurate, and complete. I am aware that there are significant penalties for submitting false information, including the possibility of fine and imprisonment for knowing violations.

_____

Mr. Bruce Ambo
City of Morro Bay

Date _____

TABLE OF CONTENTS

LIST OF FIGURES

LIST OF TABLES

INTRODUCTION

The City of Morro Bay and the Cayucos Sanitary District (MBCSD) jointly own the wastewater treatment plant operated by the City of Morro Bay. A National Pollutant Discharge Elimination System (NPDES) permit, modifying secondary treatment requirements, was originally issued to the MBCSD in March 1985. The permit was issued by Region IX of the U.S. Environmental Protection Agency (USEPA) and the Central Coast California Regional Water Quality Control Board (RWQCB). Following extensive evaluation processes, the permit has been re-issued twice, once in March of 1993 (RWQCB-USEPA 1993ab) and again in December 1998 (RWQCB-USEPA 1998ab).

As part of the current permit provisions, the previous monitoring program was modified to better evaluate short- and long-term effects of the discharge on receiving waters, benthic sediments, and infaunal communities (RWQCB-EPA 1998b). The program continued to include a requirement for receiving-water-quality monitoring performed on a seasonal basis. The four quarterly surveys are intended to record ambient water properties that approximate winter, spring, summer, and fall conditions. In keeping with seasonal synopses, this quarterly report summarizes the results of water-quality sampling conducted on 28 April 2007. Specifically, this second-quarter survey was conducted to capture ambient oceanographic conditions along the central California coast during the spring season.

The water-quality surveys also provide timely assessments of the performance of the diffuser structure in dispersing wastewater within stratified receiving waters. Any significant, recent damage to the diffuser structure would be revealed by a decline in the level of wastewater dispersion measured in this survey compared to that of prior surveys, and compared to design specifications. As described in this report, no such decline was observed in the April 2007 field survey.

Both monitoring objectives were achieved through an evaluation of the water-column profiles and cross sections of water-property distributions that are presented in Appendix A. Appendix B tabulates instrumental measurements and standard field observations. These data were used to assess compliance with the objectives of the California Ocean Plan (COP) as promulgated by the NPDES discharge permit.

The April 2007 field survey was the thirty-fourth receiving-water survey to be conducted under the monitoring provisions of the current permit. Compared to the previous permit, the number of stations increased from 11 to 16, and the stations were relocated closer (≤100 m) to the diffuser structure. Sampling at these more closely spaced stations could only be achieved because of the availability of increased navigational accuracy that resulted from implementation of the differential global positioning satellite (DGPS) system. This system was commissioned during the March 1998 survey (MRS 1998a) and was subsequently employed in the precise determination of the open section of the diffuser structure during a diver survey on 29 September 1998 (MRS 1998bc).

The current sampling design also allowed surveying to be conducted more rapidly than previous surveys by eliminating the requirement for collection of discrete water samples at individual stations. These samples were collected using Niskin bottles, which was time consuming and interrupted the continuity of instrumental measurements collected by the CTD[1] instrument package. Continuous deployment of the CTD between stations now provides a more synoptic snapshot of the water properties immediately

[1] Conductivity, Temperature, and Depth (CTD) were the original measurements recorded by this standard oceanographic instrument package, but the moniker now connotes an electronic instrument package with a broader suite of probes and sensors capable of *in situ* measurement of dissolved oxygen, transmissivity, and pH.

surrounding the diffuser structure. Consequently, the extent of the effluent plume and the amplitude of its associated water-property anomalies can be more precisely determined. The sensitive sensors onboard the CTD instrument package are capable of detecting minute changes in water properties. These sensors are described in the Methods Section below.

Surveys conducted prior to 1999 rarely detected the effluent plume because sampling stations were too widely separated to resolve a dilute wastewater signature that is highly localized around the outfall diffuser. With the implementation of the current sampling design in 1999, the presence of well-mixed effluent near the diffuser structure was found in all 34 of the subsequent water-quality surveys (MRS 2000, 2001, 2002, 2003, 2004, 2005, 2006, 2007), including the one described in this report. Moreover, improved navigation in concert with the denser sampling pattern more precisely delineated the location of the discharge-related perturbations in seawater properties.

Precision navigation is important for assessing compliance because most receiving-water limitations apply only beyond the narrow zone of initial dilution (ZID) that surrounds the outfall. Additionally, the amplitudes of the effluent-related perturbations can be better determined by the denser sampling pattern. The amplitudes of discharge-related salinity anomalies reveal the details of dilution as the effluent plume disperses within receiving waters. Measured dilution factors lend insight into the current operational performance of the outfall and diffuser structure. As described in this report, the presence of dilute effluent undergoing turbulent mixing below a strong thermocline north of the diffuser structure was delineated by the data collected during the April 2007 survey.

STATION LOCATIONS

The water-sampling stations surround the area where effluent is discharged within Estero Bay (Figure 1). The 1,450 m long outfall pipe, which carries the effluent from the onshore treatment plant, terminates at the diffuser structure, which lies on the seafloor approximately 827 m from the shoreline.[2] The diffuser structure itself extends an additional 52 m toward the northwest from the outfall terminus.

Twenty-eight of the 34 available ports discharge effluent along a 42 m section of the diffuser structure. The other six diffuser ports remain closed to improve dispersion by increasing the ejection velocity from the open ports. For a given flow rate, the diffuser ports were hydraulically designed to create an turbulent ejection jet, which serves to rapidly mix effluent with receiving seawater immediately upon discharge. Additional turbulent mixing occurs as the buoyant plume of dilute effluent rises through the water column. Most of this buoyancy-induced mixing occurs within a zone of initial dilution (ZID), whose lateral extent in modeling studies is considered to be approximately 15 m from the centerline of the diffuser structure. Beyond the ZID, the energetic waves, tides, and coastal currents within Estero Bay further disperse the discharge plume within the open-ocean receiving waters. Areas of special concern, such as sanctuaries and estuaries, are too distant to be affected by the effluent discharge. For example, the southern boundary of the Monterey Bay National Marine Sanctuary is located 38 km to the north, near Cambria Rock.

[2] This distance was determined from a navigational survey conducted on 6 July 2005 to benchmark the locations of the current surfzone sampling stations along the shoreline adjacent to the diffuser structure. The beginning of the section of the diffuser structure containing open diffuser ports lies directly offshore surfzone Station C (Figure 1). This closest-approach shoreline position was determined at the water's edge when the tidal level was +2.7 ft, referenced to mean lower low water (MLLW).

Figure 1. Regional Setting of Receiving-Water Sampling Stations within Estero Bay

Similarly, the entrance to the Morro Bay National Estuary lies 2.8 km south of the discharge and direct seawater exchange between the discharge point and the Bay is restricted by the southerly orientation of the mouth of the Bay, and by the presence of Morro Rock. Morro Rock is the largest physiographic feature of the adjacent coastline and extends into Estero Bay approximately 2 km south of the point of discharge (Figure 1). Its presence further restricts the direct exchange of seawater between the discharge point and the Bay.

Near the diffuser, prevailing currents generally follow bathymetric contours, which parallel the north-south trend of the adjacent coastline. Because of the rapid initial mixing achieved within 15 m of the diffuser structure, impingement of unmixed effluent onto the adjacent coastline 827 m away is highly unlikely. Nevertheless, water samples are regularly collected along the shoreline at the surfzone sampling stations shown in Figure 1. These surfzone samples are analyzed for total and fecal coliform levels. Results of these analyses are reported in monthly operational summaries and in annual reports. The instances of elevated beach coliform levels that are occasionally observed have resulted from onshore non-point sources rather than the discharge of disinfected wastewater from the MBCSD outfall (MRS 2000, 2001, 2002, 2003, 2004, 2005, 2006, 2007).

As shown in Figure 2, the water-sampling design consists of 16 fixed offshore stations located within 100 m of the outfall diffuser structure. The target locations of the 16 offshore sampling stations are indicated by the red ⊙ symbols in the Figure. The stations are situated at three distances relative to the center of the diffuser structure in order to capture any discharge-related trends in seawater properties. Six of the stations lie along a north-south axis at the same water depth (15.2 m) as the center of the diffuser. Stations 3 and 4 are positioned at the upcoast and downcoast boundaries of the ZID, at a distance of 15 m from the closest diffuser ports (Table 1). Stations 2 and 5 are located at nearfield distances (60 m) from the diffuser centroid. Stations 1 and 6 represent midfield stations, and are situated 100 m upcoast and downcoast of the centroid. Depending on the direction of the local oceanic currents at the time of sampling, one or more of these stations could conceivably be influenced by the discharge. Under those circumstances, the midfield station on the opposite side of the diffuser can act as a reference station. Comparisons of water properties at these antipodal stations quantify departures from ambient seawater properties so that compliance with the NPDES discharge permit can be evaluated.

Table 1. Description of Receiving-Water Monitoring Stations

Station	Description	Latitude	Longitude	Closest Approach Distance[1] (m)	Center Distance[2] (m)
1	Upcoast Midfield	35° 23.253' N	120° 52.504' W	88.4	100
2	Upcoast Nearfield	35° 23.231' N	120° 52.504' W	49.4	60
3	Upcoast ZID	35° 23.210' N	120° 52.504' W	15.0	20
4	Downcoast ZID	35° 23.188' N	120° 52.504' W	15.0	20
5	Downcoast Nearfield	35° 23.167' N	120° 52.504' W	49.4	60
6	Downcoast Midfield	35° 23.145' N	120° 52.504' W	88.4	100
7	Offshore Midfield	35° 23.199' N	120° 52.570' W	85.8	100
8	Offshore Nearfield	35° 23.199' N	120° 52.544' W	46.7	60
9	Offshore ZID	35° 23.199' N	120° 52.519' W	15.0	23
10	Shoreward ZID	35° 23.199' N	120° 52.489' W	15.0	23
11	Shoreward Nearfield	35° 23.199' N	120° 52.464' W	46.7	60
12	Shoreward Midfield	35° 23.199' N	120° 52.438' W	85.8	100
13	Southwest Nearfield	35° 23.176' N	120° 52.532' W	59.8	60
14	Northwest Nearfield	35° 23.222' N	120° 52.532' W	40.2	60
15	Northeast Nearfield	35° 23.222' N	120° 52.476' W	59.8	60
16	Southeast Nearfield	35° 23.176' N	120° 52.476' W	40.2	60

[1] Distance to the closest open diffuser port.
[2] Distance to the center of open diffuser section.

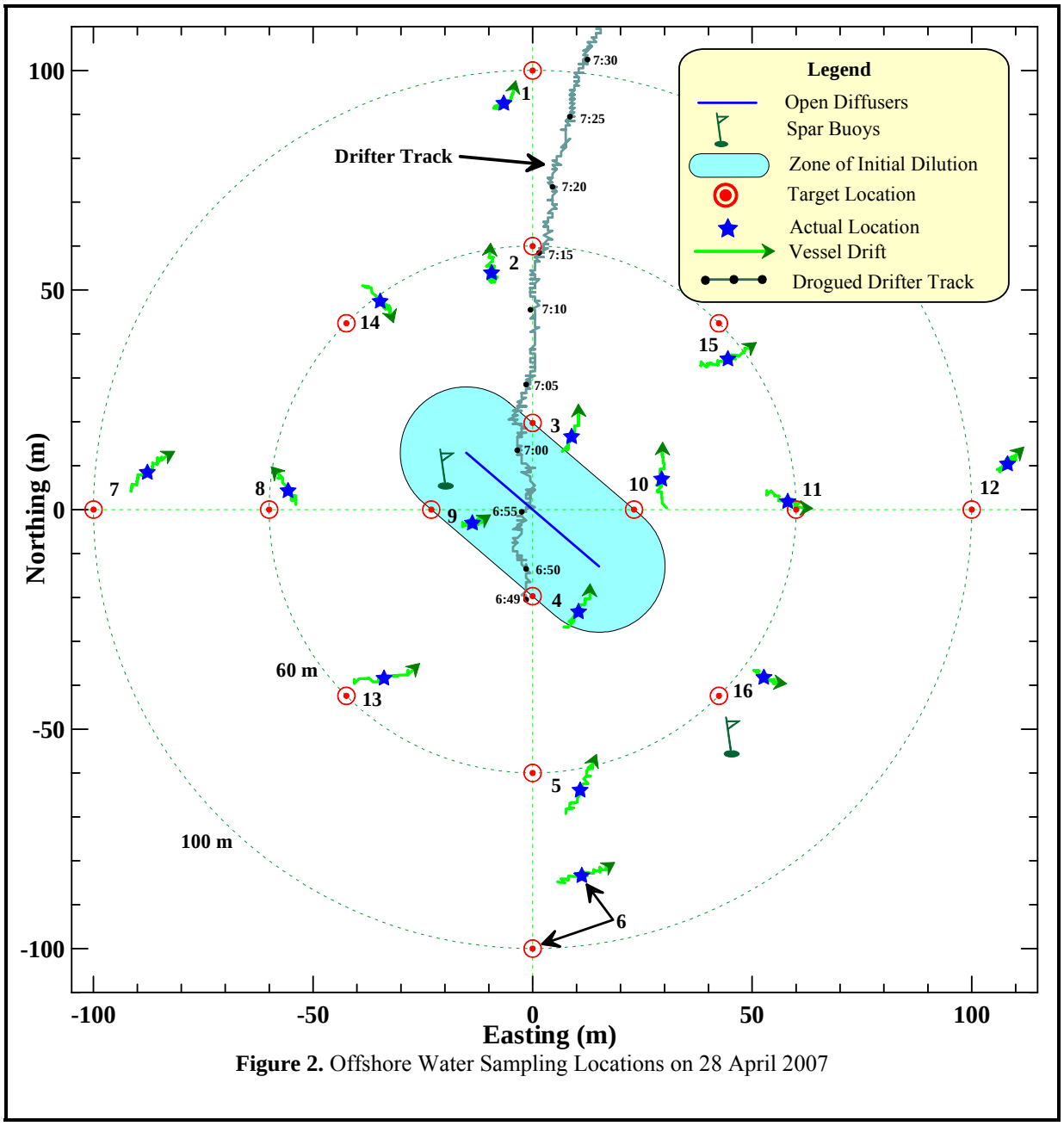

Figure 2. Offshore Water Sampling Locations on 28 April 2007

Six other stations (7 through 12) are aligned along a cross-shore transect in a pattern matching that of the along-shore transect. The remaining four stations (13 through 16) measure the nearfield influence of effluent transported by ocean currents flowing at oblique angles to the bathymetry.

An important consideration in the assessment of wastewater dispersion close to the discharge is the finite size of the diffuser. Although the discharge is considered a '*point source*,' it does not occur at a point of infinitesimal size. Instead, the discharge is distributed along a 42 m section of the seafloor. Because of this distributed discharge, the amount of wastewater dispersion at a given point in the water column is dictated by its distance to the closest diffuser port, rather than its distance to the center of the diffuser

structure. The '*closest approach*' distance can be considerably less than the centerline distance normally cited in modeling studies (Table 1).

Another important consideration for compliance evaluation is the ability to determine the actual location of the measurements. The ability to discern small spatial separations among stations within the compact sampling pattern specified in the current permit became feasible only after the advent of DGPS. The accuracy of traditional navigation systems such as LORAN or standard GPS is typically ±15 m, a span equal to half the total width of the ZID itself. Prior to 2 May 2000, standard commercial GPS receivers were not allowed to be perfectly accurate by law; and a built-in error system called Selective Availability (SA) was encoded into GPS transmissions. SA could introduce a misreading of up to 100 m, although it altered most measurements by less than 30 m. After May 2000, SA was turned off and the accuracy of standard GPS receivers improved substantially, with horizontal position errors that are now typically less than 10 m.

Even so, extreme atmospheric conditions and physiographic obstructions can still cause satellite signals to bounce around, leading to errors in position beyond those that were previously introduced by SA. These other errors are greatly reduced with the Differential GPS (DGPS) system that was first implemented by the U.S. Coast Guard to enhance offshore navigation. DGPS incorporates a second signal from a nearby, land-based beacon. Because the beacon is fixed at a known location, the position error in the reading from the GPS satellites can be precisely calculated at any given time. This correction is continuously transmitted to the DGPS receiver onboard the survey vessel and provides an extremely stable and accurate offshore navigational reading, typically with position errors of less than 2 m.

At the beginning of 1998, the survey vessel F/V *Bonnie Marietta* was fitted with a Furuno™ GPS 30 and FBX2 differential beacon receiver. This navigational system was used on 29 July 1998 to precisely locate the position of the open section of the diffuser structure (MRS 1998b) and establish the new target locations for the receiving-water monitoring stations shown in Figure 2 and listed in Table 1. The survey vessel is now fitted with two independent DGPS receivers to allow access to two separate land-based beacons for navigational intercomparison, which ensures extremely accurate and uninterrupted navigational reports.

Frequent DGPS navigational reports allow precise determination of sampling locations during the vertical CTD profiling at individual stations. Knowledge of the precise location of the actual sampling measurements relative to the diffuser position is crucial for accurate interpretation of the water-property fields. During any given survey, the actual sampling locations do not coincide with the exact target coordinates listed in Table 1. Winds, waves, and currents induce offsets during sampling. Equally important are the offsets caused by the residual momentum of the survey vessel as it approaches the target locations. Using DGPS, these offsets can be resolved and the vessel location can be precisely tracked throughout sampling at each station. This is an important consideration because vertical profiling conducted at an individual station can cover a large horizontal distance relative to the ZID.

The magnitude of the horizontal drift that occurred at each of the stations during the April 2007 survey is apparent from the length of the green tracklines in Figure 2. These tracklines trace the horizontal location of the CTD instrument package as it was lowered to the seafloor. Their lengths reflect the station-keeping difficulty experienced during the April 2007 survey. During the time it took the CTD to traverse the water column to the seafloor, which averaged 1 min 11 s, the instrument package moved as much as 13.6 m laterally. Overall, however, drift averaged 8.9 m during the survey. This amount of drift is fairly typical of most surveys.

The CTD trajectories reflect the complex interaction between surface currents, wind forces, and residual momentum as the vessel approached each station. As summarized in Table B-8, winds were light and variable during the survey. As a result, their influence was minimal compared to the northward drift induced by the prevailing current. As shown by the green tracklines in Figure 2, the drift at many of the stations had a northward component. At Stations 11, 14, and 16, the apparent southward drift of the CTD was induced either by residual momentum left after the vessel approached the station from the north, or by rotation of the vessel as it drifted northward with the current. In the former case, the influence of vessel momentum was apparent in the vessel tracklines recorded before each downcast was conducted. Although these portions of vessel track are not shown in Figure 2, the approach directions were consistent with that of the vessel drift recorded throughout each CTD cast. In the latter case, the stern of the vessel, where the CTD was deployed, rotated to the south even though the vessel centerline drifted to the north. Because the amount of drift was comparable to the 10-m vessel length, vessel rotation in response to winds affected the CTD trajectory.

Although small compared to the survey vessel's length, this magnitude of CTD drift complicated the assessment of compliance with discharge limitations at stations close to the diffuser structure. Receiving-water limitations specified in the COP only apply to measurements recorded beyond the ZID boundary. Within the ZID, rapid turbulent mixing associated with the momentum of the effluent jet and the rise of the buoyant plume is expected, and the limitations apply to conditions after this initial mixing is complete. Specifically, during the April 2007 survey, the vertical profiles at Stations 3 and 4 traversed the boundary of the ZID (Figure 2). Thus, strictly speaking, only a portion of the data recorded during these casts was subject to the receiving-water limitations specified in the NPDES discharge permit. Additionally, none of the measurements recorded at Station 9 were subject to the limitations because the CTD was well within the ZID boundary throughout the entire vertical cast at that station.

Compliance assessments notwithstanding, measurements recorded close to the diffuser structure within the ZID lend valuable insight into the outfall's effectiveness at dispersing wastewater during the April 2007 survey. Damaged or broken diffuser ports would be reflected by low dilution rates and measurements of concentrated effluent throughout ZID. Without measurements recorded within the ZID, the discharge plume might go undetected. This was the case in nearly every water-quality survey conducted prior to 1999, before the denser sampling pattern that is now in use was instituted.

Surveys prior to 1999 also predated the advent of DGPS. Consequently, the 8.9 m average drift experienced during sampling at individual stations in the April 2007 survey would not have been resolved with the navigation available prior to 1999. In fact, before 1999 sampling was presumed to occur at a single, imprecisely determined, horizontal location near each station. Federal and State reporting of monitoring data still depends on identification of a single position for all of the CTD data collected at a particular station. Thus, for regulatory reporting, and for historical consistency with past surveys, a single sampling location was also reported for each station during the April 2007 survey. These positions were based on the average locations shown for each station by the blue stars in Figure 2. The average positions are also listed in Table 2, along with their distance from the diffuser structure. However, based on the foregoing discussion, the distance between the average station position and the ZID does not imply that all the measurements at that station were subject to the receiving-water objectives in the discharge permit. For example, the 18.5 m closest-approach distance specified for Station 3 would suggest that all of the data at that station were collected outside of the ZID. In reality, as shown by the green trackline in Figure 2, the near-surface measurements at Station 3 were recorded within the ZID, where water-quality limitations do not apply.

Table 2. Average Coordinates of Vertical Profiles during the April 2007 Survey

	Time (PDT)				Closest Approach	
Station	**Downcast**	**Upcast**	**Latitude**	**Longitude**	**Range[1](m)**	**Bearing[2](°T)**
1	7:45:27	7:46:32	35° 23.249' N	120° 52.508' W	80.2	6
2	7:42:20	7:43:39	35° 23.228' N	120° 52.510' W	41.6	8
3	7:39:17	7:40:26	35° 23.208' N	120° 52.498' W	**18.5[3]**	41
4	7:34:30	7:35:44	35° 23.187' N	120° 52.497' W	**11.2[3]**	205
5	7:31:24	7:32:29	35° 23.165' N	120° 52.497' W	51.0	185
6	7:28:33	7:29:43	35° 23.154' N	120° 52.497' W	70.4	183
7	7:18:53	7:20:13	35° 23.204' N	120° 52.562' W	72.7	267
8	7:15:23	7:16:35	35° 23.201' N	120° 52.541' W	41.4	258
9	7:11:41	7:12:53	35° 23.197' N	120° 52.513' W	**11.1[4]**	221
10	7:08:09	7:09:32	35° 23.203' N	120° 52.485' W	24.5	41
11	7:04:29	7:05:34	35° 23.200' N	120° 52.466' W	45.5	71
12	7:00:37	7:01:37	35° 23.205' N	120° 52.433' W	95.9	76
13	7:23:13	7:24:37	35° 23.178' N	120° 52.526' W	51.1	221
14	7:49:39	7:50:49	35° 23.225' N	120° 52.527' W	39.8	331
15	7:54:47	7:55:48	35° 23.218' N	120° 52.475' W	55.1	41
16	7:59:01	8:00:15	35° 23.178' N	120° 52.469' W	45.1	124

[1] Distance from the closest open diffuser port to the average station position. Stations with some observations collected within the ZID are shown in bold.

[2] Direction measured clockwise in degrees from true north from the closest diffuser port to the average sampling location.

[3] Portions of the CTD (Conductivity-Temperature-Depth) cast were within the ZID boundary.

[4] All of the CTD cast was within the ZID boundary.

A satellite-tracked drifter documented the prevailing northward flow during the April 2007 survey. As in past reports, its trajectory is shown by the grey line with black dots in Figure 2. This drifter is designed to track the subsurface current, with little influence from the wind. Each dot along the drifter trackline represents a time span of five minutes. The drogued drifter was deployed near Station 4 at 06:49 PDT. The drifter was recovered an hour and twenty minutes later, at 08:09 PDT. In contrast to most other surveys, the moderate northward current rapidly carried the drifter out of the survey area. Its subsequent movement is presented in Figure 3. The trajectory shows, that throughout its deployment, the drifter's movement was comparatively constant in both speed and direction, although a weak eastward flow component developed after 07:15 PDT. During its deployment, the drifter traversed 251 m toward the north northeast (13°T) at an average speed of 5.3 cm/s or 0.1 knots.

The northward flow that was measured by the drogued drifter was consistent with the incoming (flood) tide that prevailed during the survey (Figure 4). In the absence of external influences, a flood tide normally induces a weak northeastward flow in the survey region. However, the flow is more often influenced by external processes, such as wind-generated upwelling. Figure 5 shows that upwelling conditions that began in February 2007 continued through early May, encompassing the April 2007 survey. Evidence of intense upwelling during the April 2007 survey is apparent in the in the satellite image on the cover of this report. The image was recorded on the day preceding the survey when skies were clear enough for sea-surface temperatures to be measured by infrared sensors on one of NOAA's polar orbiting satellites.

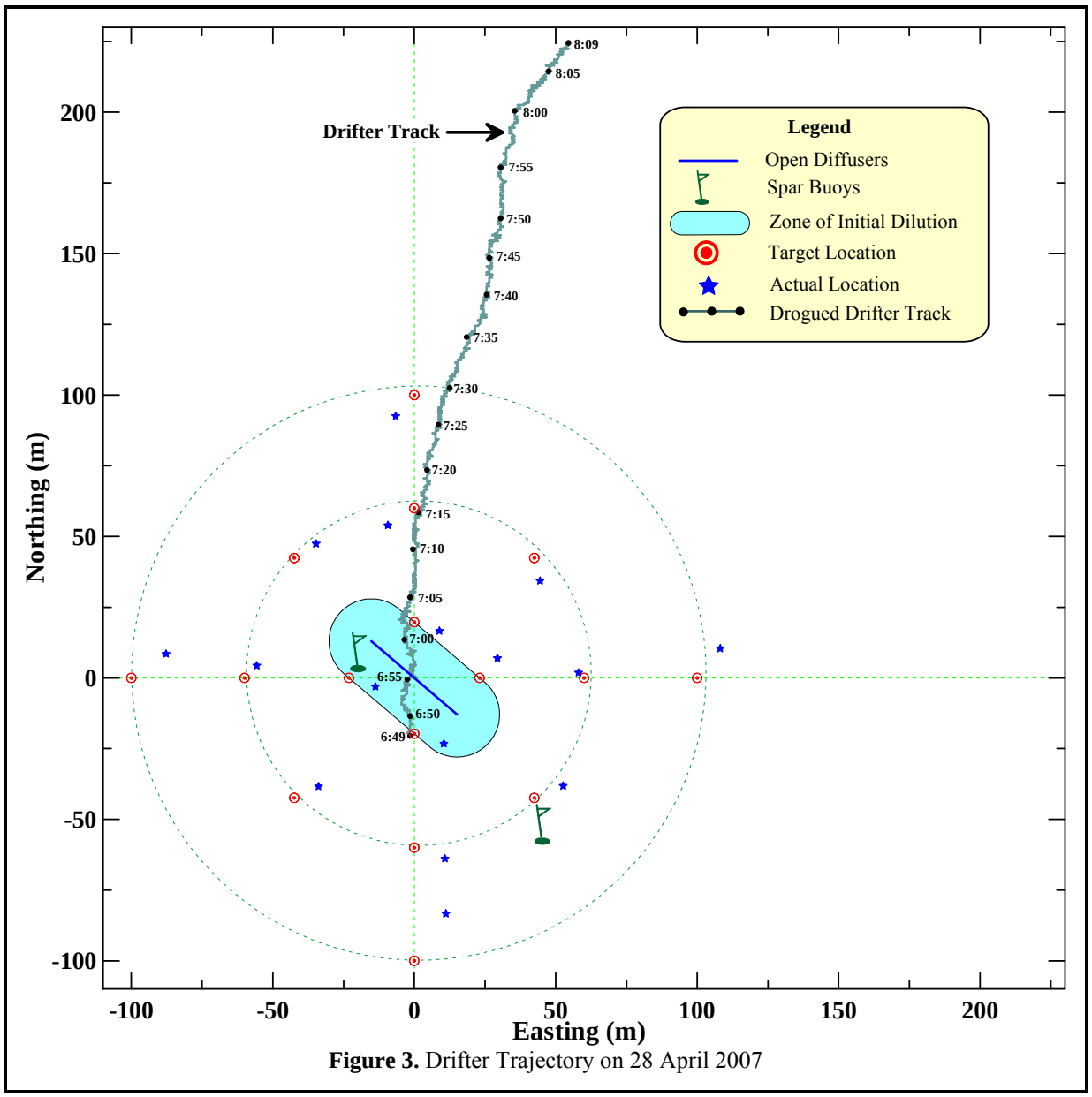

Figure 3. Drifter Trajectory on 28 April 2007

The intense upwelling that occurred around the time of the April 2007 survey was responsible for the strong water-column stratification that is evident in the vertical profiles collected with the CTD (Figures A-1 through A-3 in Appendix A). Upwelling season normally begins sometime during late March and or early April when there is a "spring transition" to more persistent southward-directed winds along the Central California Coast. This transition is marked by the stabilization of a high atmospheric pressure field over the northeastern Pacific Ocean. Clockwise winds around this pressure field drive the prevailing northwesterly winds along the Central Coast. These prevailing winds move surface waters southward and offshore. To replace these coastal surface waters, deep, cool, nutrient-rich waters upwell near the coast.

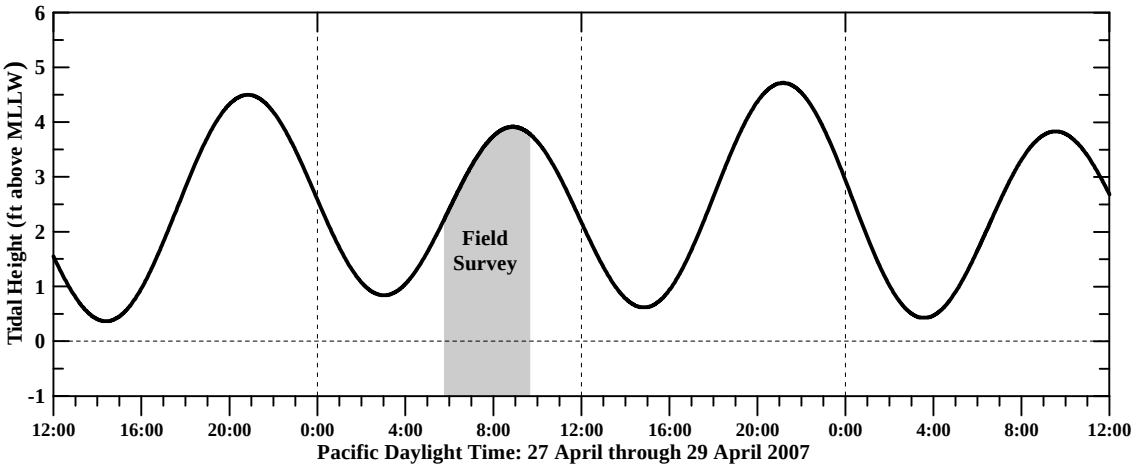

Figure 4. Estero Bay Tidal Level during the Field Survey of 28 April 2007

Strong southeastward winds along the central California coast began earlier in 2007 than in most prior years. The associated early upwelling brought some of the coldest sea surface temperatures on record to the eastern Pacific Ocean. For example, the April 2007 mean sea surface temperature (10.5°C) measured at the nearby Diablo Canyon Ocean Lab (south of Estero Bay) was 0.7°C colder than the April mean averaged over prior years. The satellite image on the cover depicts upwelling conditions with cool (11°C) sea-surface temperatures close to the central California coast and within Estero Bay, while temperatures farther offshore exceeded 12°C (light blue and green). The lower temperatures represented in the satellite image within Estero Bay were consistent with the near-surface temperatures measured by the CTD during the survey, which averaged 11.5°C (Table B-1 in Appendix B). The image also exhibits another upwelling characteristic, namely, jets of cold coastal water (dark blue and purple) extending offshore at major promontories, including Point Piedras Blancas and Pt. Arguello. These jets reflect the offshore transport of cold surface waters that were that were upwelled near the coast.

The nutrient-rich seawater that is brought to the sea surface near the coast by upwelling enables phytoplanktonic blooms that are the foundation of the productive marine fishery found along the central California coast. The cross-shore flow associated with persistent upwelling conditions also enhances vertical stratification of the water column. The shoreward transport of denser water at depth produces a shallow (<10 m) thermocline that is commonly maintained throughout summer and into the fall. In contrast, winter oceanographic conditions are normally characterized by vertically uniform conditions. Intense winds generated by passing storm fronts, and large waves produced by distant Pacific storms, generally result in a well-mixed water column in winter. In stark contrast, the vertical profiles during the April survey exhibited a sharp interface between the seawater properties within a shallow mixed layer and a deeper layer whose properties are characteristic of seawater found farther offshore in deep water. The vertical contrast in seawater properties was generated by the shoreward intrusion of offshore waters at depth.

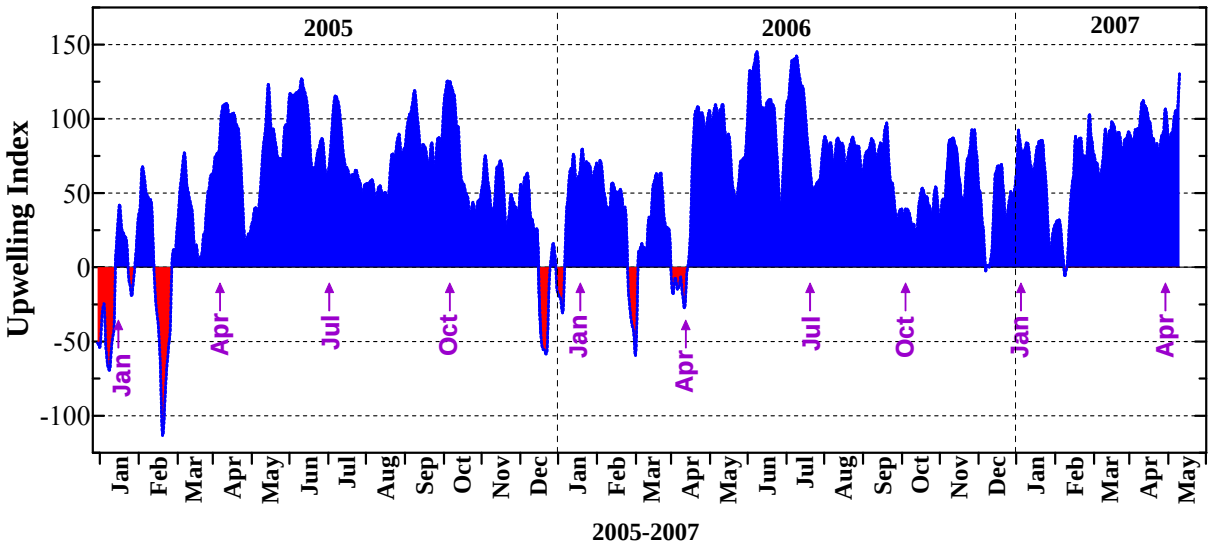

Figure 5. 30-Day Running Mean Upwelling Index ($m^3/s/100m$ of coastline) Offshore Estero Bay

METHODS

The 38 ft F/V *Bonnie Marietta*, owned and operated by Captain Mark Tognazzini of Morro Bay, served as the survey vessel on 28 April 2007. Dr. Douglas Coats of Marine Research Specialists (MRS) provided scientific support. Captain Mark Tognazzini supervised vessel operations, while Mr. Marc Tognazzini acted as marine technician. Secchi depth measurements and standard observations for weather, seas, water clarity/coloration, and the presence of any odors, floating debris, and oil and grease were recorded during the survey (Table B-8). Wind speeds and air temperatures were measured with a Kestrel® 2000 Thermo-Anemometer. These ancillary observations were collected during the rapid water-column profiling that was conducted at each station using a CTD instrument package.

Ancillary Measurements

At all stations, a Secchi disk was lowered through the water column to determine its depth of disappearance (Table B-8). Secchi depths provide a visual measure of near-surface turbidity or water clarity. The depth of disappearance is inversely proportional to the average amount of organic and inorganic suspended material along a line of sight in the upper water column. As such, the Secchi depth measures natural light penetration, which can be limited by increased suspended particulate loads from plankton blooms, onshore runoff, seafloor resuspension, and wastewater discharge. It is also of biological significance because the depth of the euphotic zone, where most oceanic photosynthesis occurs, extends to approximately twice the Secchi depth. Secchi depths of 3 m were measured at all sixteen stations during the April 2007 survey, reflecting the presence of a consistent and comparatively shallow 6-m euphotic zone. A shallow euphotic zone is typical of upwelling conditions when increased primary production, namely, increased plankton density, decreases the transmission of ambient light within the near-surface mixed layer.

Secchi depths are less precise than measurements recorded by the transmissometer mounted on the CTD instrument package. For example, the visibility of the disk, and hence its depth of disappearance, depends on the amount of natural light available at the time of the measurement. Thus, the Secchi depth reading can artificially change by as much as 0.5 m depending on whether the sample is taken on the sunny or shady side of the survey vessel. Moreover, a temporal drift in the measurements can be introduced as the sun rises in the sky while the survey progresses. Nevertheless, Secchi depth measurements reflect general turbidity levels within the upper portion of the water column, including waters within a meter of the sea surface where, because of the physical size of the CTD package, the transmissometer cannot record turbidity.

During the April 2007 survey, a satellite-tracked drifter was deployed near the open section of the diffuser structure. The drifter was drogued at mid-depth (7 m) using the curtain-shade design of Davis et al (1982). In this configuration, the drifter's trajectory was largely dictated by the oceanic flow field rather than by surface winds. The times and precise positions of the drifter deployment and recovery were recorded to determine the overall strength and direction of plume transport during the April 2007 sampling effort. In addition, the April 2007 survey was the ninth MBCSD survey to record the drifter position throughout its deployment, rather than merely calculating the average flow velocity solely from the vessel position at the time of the drifter's deployment and recovery.

Instrumental Measurements

Vertical water-column profiling was conducted using an electronic instrument package equipped with a number of probes and sensors. A Sea Bird Electronics SBE-19 Seacat CTD package was used to collect profiles of conductivity, salinity, temperature, light transmittance, dissolved oxygen (DO), pH, density, and pressure at each station. A submersible pump on the CTD continuously flushed water through the conductivity cell and oxygen plenum at a constant rate, independent of the CTD's motion through the water column. After the October 2001 survey, the CTD was returned to the factory for full testing, repair, and calibration. Temporal drifts in the oxygen and alkalinity readings during the October 2001 survey indicated that the sensitivity of these probes had degraded because of an accumulation of marine growth. During the factory repair, both the pH probe and the electrolyte in the oxygen sensor were replaced. The entire CTD system was then calibrated at the factory. Upon return of the instrument, the transmissivity, dissolved oxygen, and pH sensors were recalibrated at the MRS laboratory. Calibration coefficients determined at the factory and by MRS were nearly identical, and confirmed the accuracy and stability of the refurbished sensors.

The DO and pH sensors were again returned to the factory in May 2003 and in June 2006 for testing and calibration. Because of increasing temporal drift associated with the aging DO probe, it was replaced on both occasions with a new DO probe. As is the case before all surveys, the CTD system was recalibrated at the MRS laboratory prior to the April 2007 survey. Calibration at upper-bound DO concentrations was established by immersing the CTD in an aerated, temperature-controlled calibration tank. In addition to oxygen readings at full saturation, a zero-oxygen calibration point was determined by filling the oxygen-sensor plenum with an 8% solution of sodium sulfite (Na_2SO_3). Oxygen calibration coefficients were determined by regression analysis of sensor-membrane current and temperature, as recommended by the manufacturer (SBE 1993). As with prior factory calibrations, pre-cruise calibration coefficients determined by MRS closely corresponded to those determined by the factory.

Table 3. Instrumental Specifications for CTD Profiler

Component	Depth[1]	Units	Range	Accuracy	Resolution
Housing	600	—	—	—	—
Pump	3400	—	—	—	—
Pressure	680	Psia	0 to 1000	± 5.0	± 0.5
Depth	—	Meters	0 to 690	± 3.0	± 0.3
Conductivity	600	Siemens/m	0 to 6.5	± 0.001	± 0.0001
Salinity	600	‰	0 to 38	± 0.006	± 0.0006
Temperature	600	ºC	–5 to 35	± 0.01	± 0.001
Transmissivity	2000	%	0 to 100	± 0.1	± 0.025
Dissolved Oxygen	200	mg/L	0 to 21.5	± 0.14	± 0.014
Acidity/Alkalinity	200	pH	0 to 14	± 0.1	± 0.006

[1] Maximum depth limit in meters

The six seawater properties that were used to assess receiving-water quality in this report were derived from the continuously recorded output from the probes and sensors on the CTD. Pressure housing limitations on the combination oxygen/pH sensor confine the CTD to depths less than 200 m (Table 3), which is well beyond the maximum depth of the deepest station in the outfall survey. The precision and accuracy of the various probes, as reported in manufacturer's specifications, are also listed in Table 3. Salinity (‰) was calculated from conductivity (Siemens/m) measurements. Density was derived from contemporaneous temperature (°C) and salinity data. It was expressed as 1000 times the specific gravity minus one, which is a unit of sigma-T (σ_t).

All three of these physical parameters (salinity, temperature, and density) were used to determine the lateral extent of the effluent plume. Additionally, they define the layering (vertical stratification – stability) of the receiving waters, which determines the behavior and dynamics of the wastewater as it mixes with seawater within the ZID. Data on three remaining seawater properties, consisting of light transmittance (water clarity), hydrogen-ion concentration (acidity/alkalinity – pH), and dissolved oxygen (DO), further characterize receiving waters, and were used to assess compliance with water-quality criteria. Light transmittance was measured as a percentage of the initial intensity of a transmitted beam of light detected at the opposite end of a 0.25 m path. Increased transmittance indicates increased water clarity and decreased turbidity.

During the pre-cruise calibration, coefficients for the pH (alkalinity) sensor were determined from a linear regression of output voltage after immersion in three separate buffered solutions of known pH. Buffering solutions with a pH of 4±0.01, 7±0.01, and 10±0.02 were used to bracket the range of in situ measurements. The SeaTech transmissometer was air calibrated by fitting the voltages recorded with and without blocking of the light transmission path in air, as recommended by the manufacturer (SBE 1989). Revised calibration coefficients determined prior to the survey were used in the algorithms that converted sensor voltage to engineering units when the field data were processed. Comparison with the factory calibration of the entire CTD package that was conducted in December 2001, and the more recent June 2006 replacement and calibration of the DO probe, confirmed the continued accuracy and stability of the temperature, pressure, and conductivity sensors, as well as the operational integrity of the oxygen and pH probes.

Before deployment at the initial station, the CTD was held below the sea surface for a six-minute equilibration period. Subsequently, the CTD was raised to within 1.0 m of the sea surface and profiling commenced. The CTD was lowered at a continuous rate of speed to the seafloor. Measurements at all the stations were collected during single deployment of the CTD package by towing it below the water surface while transiting between adjacent stations. Upon retrieval of the CTD, the profile data were downloaded to a portable computer and examined for completeness and range acceptability.

Temporal Trends in the pH Sensor

The pH sensor exhibited a temporal drift during the April 2007 survey. Perceptible drift in pH measurements has been consistently observed in prior water-quality surveys as the result of ongoing sensor equilibration during profiling. Prolonged exposure to the atmosphere between surveys results in the largest offsets and can also affect the dynamic range of the measurements. During past surveys, smaller equilibration offsets were also observed when the CTD was redeployed after being brought onboard to download data during the middle of the survey. Use of a single deployment during the April 2007 survey obviated the need for mid-survey adjustments for pH drift. Previous additional attempts to mitigate sensor drift have included prolonging the soak time of the CTD prior to profiling. Soak times of six minutes at the beginning of a survey were found to reduce, but not entirely eliminate sensor drift. During the April 2007 survey, a tube filled with seawater was placed around the pH sensor while in transit to the survey site to limit atmospheric exposure of the probe prior to deployment. This technique was successful at further ameliorating sensor drift.

Despite these precautions, temporal drift in the pH sensor was responsible for perceptibly lower pH measurements at stations occupied during the initial stages of the CTD deployment. Beginning with Station 12, where the offset was -0.175 pH units, equilibration-related reductions in pH became steadily smaller as the survey progressed sequentially from Station 11 (-0.128 pH) through Station 2 (-0.006 pH). The pH measurements collected at the last four stations were stable and did not exhibit a perceptible offset. The magnitude of the pH offset at the twelve previous stations was determined by comparing pH values recorded at the sea surface with the surface pH measured at the last four stations, where the sensor was fully equilibrated.

Removal of the artificial pH trend was important because it was large compared to reported accuracy and precision of the probe. As a result, they could potentially mask very slight discharge-related anomalies. The artificial pH reduction (-0.175 pH) at the beginning of the deployment was almost double the instrumental accuracy (±0.1 pH) reported by the probe manufacturer (Table 3). Equilibration-related offsets only became smaller than the instrumental resolution (±0.006 pH) after sampling at Station 2. Before correction, equilibration-related offsets induced an artificial lateral gradient in the cross-shore transect which appears in Table B-7 as a progressively decreasing surface pH between Stations 7 and 12. As shown in Table B-6, temporal detrending effectively removed this artificial gradient.

RESULTS

The second-quarter water-quality survey began on Saturday, 28 April 2007, at 06:49 PDT with the deployment of the drogued drifter. Subsequently, all water-column measurements were collected as required by the NPDES monitoring program (Table 2 and B-9). The survey was conducted later in the month than normal because sea conditions were too rough throughout most of April 2007. This was largely due to strong sustained northwesterly winds that also induced intense upwelling in the weeks prior to the survey. Sunrise was at 06:15 PDT and skies were mostly clear throughout the survey, which ended at 09:20 PDT when the vessel returned to port.

Light and variable winds prevailed throughout the survey. Average wind speeds, calculated over one-minute intervals, ranged from 1.1 kt to 2.8 kt, with peak speeds ranging from 2.2 kt to 6 kt. Additionally, a 3 to 4 ft swell moved through the survey area from the west. Initially, surface atmospheric visibility was less than 2 nM along the ocean surface owing to the presence of low-lying haze. As a result, the shoreline was not visible until later in the survey, although Morro Rock and the power-plant stacks were visible at all times.

Air temperatures did not steadily increase as the survey progressed, as is typical during morning surveys, when increasing insolation from the rising sun warms the air. Instead, cool breezes from onshore canyons occasionally resulted in a reduction in air temperature at some of the stations. The near-surface seawater temperature (11.4°C) in the survey area was consistently lower than the coldest measured air temperature (12.6°C). The seawater temperatures measured in the upper water column during April 2007 survey were consistent with the coastal sea-surface temperatures within Estero Bay recorded by the satellite image shown on the cover of this report.

The discharge plume was not visible near the sea surface at any time during the survey. Throughout the survey, there was also no visual evidence of floating particulates, oil and grease, or seawater discoloration associated with the discharge.

Beneficial Use

During the April-2007 survey, few beneficial uses were observed compared to previous surveys. Nevertheless, one unmistakable observation occurred when a juvenile whale surfaced next to the survey vessel within the ZID during collection of the second profile at Station 4. The incident was brief and unexpected, making a species identification problematic. However, given the time of year, nearshore location of the sighting, and relative size of the whale, it was likely a juvenile gray whale (*Eschrichtius robustus*),. Gray whales are a common sighting along the California coastline in the spring months as they make their way north from breeding and calving grounds off the coast of Mexico to feeding grounds in the Bering and Chukchi seas. This northbound migration generally peaks in March but often continues into May. During 2007, whales were still seen heading north offshore Piedras Blancas during the third week of May. The majority of gray whales are found close to shore over continental shelf waters (Herzing and Mate 1984; Reilly 1984; Rice et al. 1984; Rugh 1984; Dohl et al. 1983; Sund and O'Connor 1974).

In addition to the whale sighting, a small harbor porpoise (*Phocoena phocoena*) was observed by the buoy that marks the entrance to Morro Bay during transit to the survey site. No other evidence of beneficial use of receiving waters was noted during the survey.

Ambient Seawater Properties

Data collected during the April 2007 survey reflected strongly stratified conditions that indicate that intense upwelling conditions were present at the time of the survey. Upwelling results in an influx of dense, cold, saline water at depth that normally leads to a sharp thermocline, halocline, and pycnocline where temperature, salinity, and density change rapidly over short vertical distances. Under heavily stratified conditions, isotherms crowd together to form a thermocline that restricts the vertical transport of the effluent plume and reduces its dispersion.

Strong upwelling-induced vertical gradients are plainly evident between depths of 3 m and 8 m in all sixteen vertical profiles shown in Figures A-1 through A-3. Across that 5-m interface, changes in temperature, DO, pH, and density encompassed a substantial portion of the overall range in those properties. Temperature (red lines), DO concentrations (dark blue lines), and pH (olive lines) decreased by 1.5°C, 2.2 mg/L, 0.13 pH units, while density (black lines) increased by $0.25\sigma_t$. The changes in DO, pH, and density account for about half of the overall range in those properties observed in the April 2007 survey, and 75% of the observed temperature range.

The vertical contrast in these seawater properties resulted from the juxtaposition of two watermasses. Within the 3-m surface mixed layer, wind-induced stirring created a relatively uniform slab of water that was warmed by insolation. DO concentrations within this uniform surface watermass were close to saturation from rapid equilibration with the overlying atmosphere, and from primary production (photosynthesis) by phytoplankton that thrive on the nutrients that were brought close to the surface by upwelling. The contrasting seawater characteristics of the watermass below the thermocline reflect its deeper offshore origin. Upwelling moved this cold, dense, watermass shoreward from great depths to replace the nearshore surface waters that were driven offshore by southeastward winds. Within this deep watermass, DO concentrations were comparatively low because photosynthesis was limited to the 6-m euphotic zone, and because biotic respiration and decomposition had slowly depleted oxygen levels in the watermass during the long period since its contact with the atmosphere. Biotic respiration and decomposition also produced dissolved CO_2 (carbonic acid), which resulted in measurably lower pH (more acidic) levels within the watermass.

Other physicochemical processes determined the shape of the vertical profiles of transmissivity (light blue lines) and salinity (green lines). Within the 6-m euphotic zone, the increased phytoplankton abundance resulted in an increase in turbidity. Consequently, light transmissivity within this shallow layer was consistently lower than in the seawater within most of the deep watermass, except very close to the seafloor. At all stations, the vertical profiles of transmissivity exhibited a sharp decrease within about 4 m of the seafloor. This resulted from the presence of a bottom nepheloid layer (BNL), which is a widespread phenomenon on continental shelves (Kuehl et al. 1996). The increased turbidity observed within the BNL is caused by the presence of naturally occurring particulates formed from light-weight flocs of detritus. This detritus is easily suspended by oscillatory bottom currents generated by passing surface gravity waves. The vertical profiles demonstrate that the turbidity within the BNL is often much larger than the turbidity associated with the near-surface euphotic zone. Regardless, the increased particulate loading within these two layers produced a localized, mid-depth transmissivity maximum at most stations during the April 2007 survey.

In contrast to the other water properties, the vertical profiles of salinity (green lines) do not exhibit a distinct halocline. Normally, a halocline would be expected in conjunction with the upwelling-induced thermocline. Specifically, average salinity is expected to be slightly higher near the seafloor than at the sea surface. The expected salinity increase at depth reflects the shoreward transport of a deep water-mass

that originated in the more saline waters to the south. However, subtle vertical trends in salinity are difficult to discern because of the presence of large salinity spikes within the thermocline. Salinity spikes are instrumental artifacts arising from the mismatch between conductivity and temperature measurements collected near strong thermal gradients. The spikes are evident as erroneous zigzag patterns, or localized salinity decreases that appear in conjunction with sharp changes in temperature. The erroneous spikes are often also reflected in the vertical density profiles (black lines). In the vertical profiles shown in Figures A-1 through A-3, the salinity spikes mask the presence of slightly higher salinity near the seafloor as compared to the sea surface.

Lateral Variability

Normally, the influence of the effluent discharge can be best identified from localized anomalies in seawater properties, particularly salinity. In contrast to the vertical profiles, discharge-related anomalies become especially apparent in cross sections because they highlight differences in seawater properties at adjacent stations. However, in the April 2007 survey, the presence of large salinity spikes confounded the interpretation of the comparatively small salinity changes that would have been generated by the presence of dilute effluent. Similarly, oscillations in the thickness of the bottom nepheloid layer (BNL), and differences in the height of the CTD measurement within this layer, produced lateral anomalies in transmissivity that were unrelated to the discharge.

Nevertheless, as in past surveys, cross sections of all six seawater properties were examined both visually and statistically for lateral anomalies that could potentially be associated with the wastewater discharge. Figures A-4 and A-5 depict the lateral variability along a transect that paralleled the shoreline, while Figures A-6 and A-7 document trends in seawater properties along a transect perpendicular to the coast. In addition, the significance of each potential discharge-related anomaly was statistically evaluated by comparing its amplitude to natural background variability. Each observation at a particular station was compared with the observations from other stations at the same depth level. Measurements recorded within 10 m of the sea surface were compared with other measurements at the same depth level below the sea surface. However, deeper measurements were compared with other measurements recorded at the same height above the sloping seafloor. These different depth references are used because deep seawater properties tend to parallel the sloping seafloor rather than the horizontal sea surface. Similarly, measurements within the thermocline were compared to adjacent measurements at the same thermocline level. Again, this is because the depth of the thermocline varied slightly among the stations, and seawater properties tend to track the thermocline depth rather than the sea surface.

The statistical significance of departures from ambient seawater properties was computed from the raw CTD data listed in Tables B-1 through B-7. First, anomalies from mean conditions were computed by subtracting a particular measurement from the average of all other measurements at the same depth level, whether measured relative to the sea surface, the thermocline, or the seafloor. Natural variability was then estimated from the standard deviation of all measurements (excluding the one in question) for a given seawater parameter (e.g., salinity). Statistically significant anomalies were those that departed from mean conditions by more than the 95% confidence interval, which is determined from the standard deviation and number of observations used to compute the average. Statistically significant departures from ambient conditions are highlighted in Tables B-1 through B-7 by bold typeface enclosed in boxes.

Only three of the six of the seawater properties exhibited statistically significant departures from mean conditions, as shown in Tables B-2 (salinity anomalies at Stations 3, 6, and 16), B-3 (density anomaly at

Station 3), and B-5 (transmissivity anomalies near the seafloor at seven stations). It is unlikely that the discharge was responsible for the statistical significance of any of the highlighted departures except for the transmissivity anomaly near 12 m at Station 10. Excluding this anomaly, and the physically interrelated reductions in salinity and density near 5 m at Station 3, the other significant anomalies were not spatially coincident. Normally, the signature of the discharge is apparent in several seawater properties at once. Moreover, as shown in Figure 2, Stations 6, 11, 12, 13, and 16 were not located in the northward transport path of the plume. Lastly, the positive (increased) salinity anomaly at Station 16 (Table B-2), and the positive (increased) transmissivity near the seafloor at Stations 1, 10, and 12 (Table B-5) are not consistent with the presence of wastewater constituents. Wastewater is both less-saline and more-turbid than ambient seawater.

The statistical significance of these anomalies was an artifact of either salinity spiking or variations in the thickness of the BNL. Statistical tests for lateral differences in transmissivity near the seafloor randomly identified several significant anomalies because a sharply defined BNL was present during the April 2007 survey. The BNL generated large lateral transmissivity differences as a result of slight differences in the height of the associated turbidity interface above the seafloor. In April 2007, variations in the BNL measurements produced all of the statistically significant transmissivity anomalies highlighted in Table B-5 except one. As expected from their relationship to the BNL, all the transmissivity anomalies were close to the seafloor. In addition, both positive and negative anomalies were identified, as would be expected when differences in the thickness of the BNL among stations are present.

The transmissivity anomalies are further enhanced by differences in CTD's penetration into the BNL. The reported measurements are averages of CTD readings over a 0.5-m depth interval, an interval that encompassed a substantial portion of the thin BNL that extended above the seafloor during the April 2007 survey. Consequently, the details of the vertical variation of turbidity within the BNL were not well-resolved by the depth-averaged measurements. This resulted in artificial lateral differences in the transmissivity reported for the deepest portion of the CTD casts. Such a difference is apparent from a comparison of the deepest part of the transmissivity profiles at Stations 1 and 2 (light blue lines in the two top frames of Figure A-1). At Station 1, incomplete resolution of the BNL turbidity resulted in a statistically significant positive anomaly for the deepest transmissivity measurement (Table B-5). In contrast, the deepest reported transmissivity value at Station 2 captured more of the BNL turbidity, resulting in a statistically significant negative anomaly.

Even in the absence of a distinct BNL, the presence of statistically significant fluctuations unrelated to the discharge is expected from the nature of statistical hypothesis testing itself. From the definition of a 95% confidence level, one '*significant*' departure out of every 20 measurements should occur by chance alone. With 500 measurements examined for each of the six parameters, it would not be surprising if a random few departed from the mean by an amount more than the 95% confidence interval. Moreover, when multiple hypotheses are being tested (*i.e.*, one for each observation), the error rate for each individual test should be adjusted to achieve the overall experimentwise error rate of 5% (95% confidence). By definition, this error rate is the probability that one or more of the hypothesis tests would incorrectly find a significant difference when none exists. Thus, without correcting for repeated hypothesis testing, the individual tests are conservative and "*significant*" departures will be found more often than if a single test were being performed at the 95% confidence level.

The only other statistically significant anomalies found during the April 2007 field survey occurred in the salinity field (Stations 3, 6, and 16 in Table B-2) and in the density field (Station 3 in Table B-3). Density is computed from salinity, so the statistically significant density anomaly at 5 m at Station 3 was a direct result of the large salinity anomaly reported at that location. As such, the density anomaly does not represent an independent observation. As with the transmissivity anomalies, the reported statistical significance of the salinity (and density) anomalies was artifactual, rather than an actual excursion of seawater properties related to the presence of effluent constituents. However, in contrast to the BNL variations, these anomalies arose from instrumental artifacts known as salinity spiking. Salinity spiking is a common occurrence in CTD measurements collected within upper-ocean thermoclines, and is routinely observed in MBCSD surveys conducted when the water column is well stratified (MRS, 2001, 2002, 2003, 2004, 2005, 2006, 2007). Salinity spiking occurs when the CTD package crosses a strong thermocline. Salinity is computed from conductivity and temperature probes that are physically separated from one another on the CTD. In addition, the sensors do not have the same response times so even if they are close together, they will not simultaneously report data from same water parcel. Consequently, when encountering an abrupt temperature change, the mismatch between the conductivity and temperature readings results in erroneous spikes in the reported salinity. The sharper the thermal gradient, the larger the salinity spike.

During the April 2007 survey, erroneous spikes were apparent at most stations as localized reductions in salinity near a depth of 5 m. These are delineated in red and green in the salinity cross sections shown in the top frames of Figures A-4 and A-6. However, these cross sections are smoothed versions of the actual individual CTD measurements. The spikes were actually larger and more localized than depicted in the Figures. As discussed above, the figures and tables presented in this report were based on CTD measurements averaged over 0.5-m depth intervals. Although not shown here, high-resolution vertical profiles of raw temperature and salinity data were reviewed for evidence of salinity spiking. Those profiles distinctly characterized the highly localized outliers in salinity that only occurred within limited regions of the thermocline where there were very abrupt temperature changes. However, because they were generally less than 0.5 m thick, they appear as weaker, vertically distributed features in the lower-resolution salinity profiles included in this report (green lines in Figures A-1 through A-3).

The largest salinity spike, by far, occurred at a depth of 5 m at Station 3. Its unusually large magnitude is apparent in the salinity (green line) and density (black line) profiles shown in the middle-left frame of Figure A-1. It was much larger than the spike at other stations because the vertical temperature change (red line) was much more abrupt at Station 3 than at other stations. The highly compressed thermocline is also apparent in the middle frame of Figure A-4 as increased crowding of isotherms near 5 m at Station 3. The vertical extent of the thermocline was compressed at Station 3 by the rising effluent. However, although plume dynamics caused the compression, effluent constituents were too dilute to account for the large magnitude of the salinity anomaly observed at that location. On the contrary, the rising effluent plume pushed colder seawater from near the seafloor ahead of it as it rose into the upper water column. This reduced the thickness of the thermocline to only 2 m, which is only about half the thickness found at the other monitoring stations. As a result of the sharper thermal gradient at Station 3, the amplitude of the salinity spiking was much more pronounced at this location than at other stations.

Table 4. Discharge-Related Water-Property Anomalies[a]

Perturbation[b]	Station	Depth Range	Depth of Extremum	Property	Magnitude	Mechanism
P1 Dilution Indeterminate[c]	3	5.0 to 5.5 m	**5.0 m**	**Salinity**	**–0.247 ‰**[d]	Spike
		5.0 m	**5.0 m**	**Density**	**–0.272 σ_t**[d]	Spike
		4.5 to 8.0 m	5.5 m	Temperature	–0.84 ºC [e]	Entrainment
		4.0 to 10.0 m	9.0 m	Transmissivity	–5.9 %	Entrainment
P2 Dilution ≥ 557:1	10	8.5 to 11.0 m	10.0 m	Salinity	–0.064 ‰	Effluent
		7.0 to 13.5 m	**12.0 m**	**Transmissivity**	**–13.0 %**	Entrainment
		7.0 to 10.5 m	9.0 m	Dissolved Oxygen	–0.53 mg/L	Entrainment

[a] Anomalies shown in bold type were statistically significant

[b] Perturbations are composed of a group of spatially consistent anomalies in several different seawater properties

[c] The computed dilution of 136:1 was confounded by a salinity spike in the instrumental measurements (see the discussion in the text)

[d] The magnitudes of the reported negative salinity and density anomalies were artificially increased by a salinity spike

[e] Relative to other measurements at the same level within the thermocline

Discharge-Related Perturbations

Despite the confounding influence of salinity spiking and the influence of BNL variations during the April 2007 survey, two distinct perturbations in seawater properties were related to the discharge (Perturbations P1 and P2 in Table 4). A discharge-related perturbation is a group of anomalies in one or more seawater properties that are spatially contiguous at a particular station. The vertical distribution of seawater properties within and below the perturbations lends insight into which of two discharge processes were responsible for generating a particular anomaly. Discharge-related anomalies are either induced by the properties of dilute wastewater constituents, or are generated by the upward displacement ambient seawater that is entrained in the rising effluent plume. Wastewater-induced anomalies only occur when the contrast between the properties of wastewater and seawater are large enough to remain apparent after rapid initial dilution. Because of the large difference between wastewater and seawater salinity and density, wastewater-induced anomalies are usually only apparent in those two fields. Similarly, entrainment-generated anomalies are only apparent when the water column is stratified and the juxtaposition of deep seawater properties carried upward in the rising effluent plume provides a contrast with shallow seawater properties.

The mechanism that produces discharge-related anomalies is an important consideration when assessing the discharge's compliance with the receiving-water objectives of the COP, and the requirements of the NPDES permit. As indicated in Table 4, only the salinity and density anomalies reflected the presence of dilute wastewater, while the anomalies in other water properties were generated by entrainment of ambient seawater within the rising effluent plume. Because the thermal, transmissivity, and DO anomalies reflect the properties of ambient seawater that has been displaced upward, they are not subject to water-quality restrictions that were developed to limit the discharge of wastewater contaminants.

Regardless of the processes that produced the anomalies, and irrespective of their statistical significance, the two perturbations listed in Table 4 were related to the discharge for the following reasons.

- Anomalies in several different seawater properties co-occurred spatially.
- Stations 3 and 10 were in comparatively close proximity to the diffuser structure (Figure 3).
- Stations 3 and 10 were located north of the diffuser structure along a path where the prevailing current was likely to carry the effluent plume.
- Transmissivity anomalies at Stations 3 and 10 (top frames of Figures A-5 and A-7) were consistent with the upward displacement of turbid seawater within the BNL into a mid-depth layer that had naturally high seawater clarity.
- The DO anomaly at Station 10 (middle frame of Figure A-7) is also consistent with entrainment of ambient bottom water, which is naturally depleted in oxygen, within the rising effluent plume.
- The salinity anomaly observed near 10.0 m at Station 10 was well below the 6.5 m base of the thermocline, and therefore, was not an artifact of salinity spiking.

The vertical separation between the discharge-related salinity anomaly at Station 10 and the overlying salinity spike is blurred by depth averaging in the top frame of Figure A-6. Instead, the presence of the discharge-related reduction in salinity is apparent as a downward elongation of the 33.98‰ salinity contour. In contrast, the much larger salinity spike at Station 3 completely overwhelms any discharge-related reduction in salinity. Nevertheless, the compression of the isotherms at Station 3, along with the presence of a small transmissivity anomaly in the upper water column indicates that entrainment contributed to discharge-related Perturbation P1.

Initial Dilution Computations

The amplitude of negative salinity anomaly at Station 10 lends insight into effectiveness of the outfall at dispersing effluent and, ultimately, compliance with the receiving-water objectives of the COP and NPDES discharge permit. The critical initial dilution applicable to the MBCSD outfall was conservatively estimated to be 133:1 (Tetra Tech 1992). This estimate was based on worst-case modeling using highly stratified conditions where the trapping of the plume below the thermocline limited the mixing achieved during the buoyant plume's rise through the water column. The dispersion modeling determined that, after initial mixing was complete, 133 parts of ambient water would have mixed with each part of wastewater. The modeling predicted that this dilution would be achieved after the plume rose only 9 m from the seafloor, whereupon it would become trapped below a thermocline and spread laterally with no further substantive dilution. A 9-m rise translates into a trapping depth that is 6.4 m below the sea surface.

However, as described below, dilutions computed from the salinity anomaly observed at Station 10 during the April 2007 survey demonstrated that the effluent plume actually achieved a far higher dilution (>557:1) at depths (10 m) well below the predicted trapping depth (6.4 m). The conservative nature of the dilution ratio determined from modeling is an important consideration because it was used to specify permit limitations on chemical concentrations in wastewater discharged from the treatment plant. These end-of-pipe effluent limitations were back-calculated from the receiving-water objectives listed in the COP (SWRCB 1997) using the 133:1 dilution ratio determined from the modeling. Use of a higher critical dilution ratio would relax the stringent end-of-pipe effluent limitations that were thought to be necessary in order to meet Ocean-Plan standards.

End-of-pipe limitations on contaminant concentrations within effluent were based on the definition of dilution (Fischer et al. 1979). From the mass-balance of a conservative tracer, the concentration of a particular contaminant within effluent before discharge (C_e) can be determined from Equation 1.

$$C_e \equiv C_o + D\left(C_o - C_s\right) \qquad \textbf{Equation 1}$$

where: C_e = the concentration of a constituent in the effluent,
C_o = the concentration of the constituent in the ocean after dilution by D (*i.e.,* the COP objective),
D = the dilution ratio of the volume of seawater mixed with effluent, and
C_s = the background concentration of the constituent in ambient seawater.

By rearranging Equation 1, the actual dilution achieved by the outfall can also be determined from measured seawater anomalies. This measured dilution can then be compared with the critical dilution factor determined from modeling. Salinity is an especially useful tracer because it directly reflects the magnitude of ongoing dilution. Specifically, the salinity concentration in effluent is negligible so C_e is eliminated in Equation 1 and the dilution ratio (D) can be computed from the salinity anomaly ($A = C_o - C_s$) as:

$$D = \frac{-C_o}{\left(C_o - C_s\right)} \equiv \frac{-C_o}{A} \qquad \textbf{Equation 2}$$

where: D = the dilution ratio of the volume of seawater mixed with effluent,
C_o = the salinity of the effluent-seawater mixture after dilution by D,
C_s = the background seawater salinity (approximately 32.9‰), and
$A = C_o - C_s$ = the salinity anomaly.

The magnitude of the salinity anomaly at Station 10 (–0.064‰) was used in Equation 2 to compute the dilution level listed in the first column of Table 4 for Perturbation P2. This demonstrates that the modeled dilution factor (133:1) was significantly more conservative than the actual dilution achieved by the discharge during the April 2007 survey. Specifically, the minimum dilution computed from the largest discharge-induced salinity anomaly exceeded 557:1. Furthermore, this salinity anomaly was recorded 10 m below the sea surface at Station 10, and it is likely that additional dilution would be achieved as the effluent plume rose farther upward in the water column. The measured dilution that was four times higher than the dilution predicted by modeling, and was at a depth that was 3.6 m deeper than the trapping depth predicted by modeling. Theoretically, the dilution should be lower than the model predictions at this depth because the effluent plume had not experienced as much buoyancy induced dispersion as predicted by modeling.

Extreme salinity spiking at Station 3 overwhelmed any effluent-induced reduction in salinity, and precluded the computation of dilution within Perturbation P1. As described previously, the salinity spiking at Station 3 was particularly severe because the cool seawater carried upward with the rising effluent plume further compressed the already steep thermocline. As a result, a very large magnitude (–0.247‰) salinity anomaly was reported. However, little of this erroneously large anomaly could be ascribed to the presence of wastewater constituents. Perturbation P1 was located at Station 3, which was approximately the same distance from the diffuser structure as Station 10 (Figure 2). Both stations were located north of the discharge, and in line with the transport direction of the effluent plume. Given the shallower depth of the Station-3 anomaly, one would expect the discharge-induced salinity reduction to be less than the one at Station 10. Based on these comparisons, spiking within Perturbation P1 increased the

amplitude of the salinity anomaly by at least a factor of four compared to the anomaly that would have been produced by the presence of dilute wastewater constituents alone.

The unrealistically large amplitude ($-0.272\sigma_t$) of the density anomaly associated with the salinity spike within Perturbation P1 provides additional evidence that the presence of effluent constituents could not have materially contributed to the spike. The negative density anomaly created a large, artificial inversion, wherein a highly buoyant parcel of water was surrounded by much denser ambient seawater. However, under natural oceanic conditions, even small instabilities almost never occur. This is because seawater overturn takes place rapidly. The associated turbulent mixing maintains a universally stable water column with steadily increasing density with increasing depth. Thus, an inversion such as that suggested by the density anomaly would be an extraordinarily unlikely and transient feature. Instead, the density anomaly within Perturbation P1, along with the associated salinity anomaly, was an artifact of salinity spiking.

In contrast, the 557-fold dilution determined for Perturbation P2 provides an accurate portrayal of the performance of the diffuser structure during the April 2007 survey. The computed dilution was four-times the level predicted by the modeling. This demonstrates that, during the April 2007 survey, the outfall was performing better than designed, and was rapidly diluting effluent more than 500-fold beyond the boundary of the ZID. With this level of dilution, the COP receiving-water objectives were easily met by the chemical concentration limits promulgated by the NPDES discharge permit issued to the MBCSD.

DISCUSSION

Sampling during the April 2007 survey indicated that the wastewater discharge was in compliance with the receiving-water limitations specified in the NPDES permit, and with the water-quality objectives of the COP (SWRCB 1997) and the Central Coast Basin Plan (RWQCB 1994). Specifically, there were no particulates of sewage origin seen floating on the ocean surface at any of the stations sampled during the April 2007 water-quality survey, and the discharge complied with all quantitative limits on seawater properties.

Although discharge-related changes in four of the six water properties were observed during the April 2007 survey, the changes were either not statistically significant, were measured in parameters not regulated by the discharge permit, were located below the euphotic zone, or resulted from the displacement of ambient seawater rather than the presence of effluent constituents. Other than the erroneous salinity and density anomalies at Station 3 (Perturbation P1), the transmissivity anomaly within Perturbation P2 at Station 10 was the only statistically significant change in seawater properties that could potentially be related to the discharge. However, this localized reduction in transmissivity was generated by the upward displacement of naturally turbid seawater within the BNL, rather than the presence of wastewater particulates. This was also true of the transmissivity anomaly at Station 3 (Perturbation P1), which was not statistically significant.

The transmissivity cross section in the top frame of Figure A-7 shows how the distribution of ambient turbidity during the April 2007 survey favored the generation of entrainment anomalies. The figure delineates a highly turbid BNL near the seafloor with red and green shading. Wastewater is rapidly diluted 100-fold upon ejection from the diffuser ports by turbulent mixing with seawater near the seafloor. Thus, shortly after discharge, the dilute effluent plume acquires the characteristics of the ambient seawater near the seafloor, in this case, the naturally high turbidity within the BNL. As the buoyant effluent plume rose in the water column near Station 10, its increased turbidity contrasted with the naturally high seawater clarity of the mid-depth watermass, and generated the lateral turbidity anomalies associated with

Perturbation P2. The same entrainment mechanism was responsible for the increased mid-depth turbidity at Station 3 that is apparent in the top frame of Figure A-5 (Perturbation P1).

These transmissivity anomalies would not have been present without a naturally occurring vertical contrast in turbidity. A dilution computation using Equation 1 demonstrates that effluent particulates could not have materially contributed to the reduced transmissivity associated with the Perturbations. Under conditions of uniformly low ambient seawater turbidity comparable to that of the mid-depth watermass, and a dilution of at 557-fold (Perturbation P2), wastewater particulate concentrations of 20 mg/L measured at the treatment plant around the time of the survey would be reduced to 0.03 mg/L within the effluent plume. Based on transmissometer calibrations, this would induce a drop in transmissivity of only about 0.2%, which is not only two orders of magnitude smaller than the observed anomaly (13%), but it is also very close to the 0.1% resolution capability of the transmissometer (Table 3).

Outfall Performance

A small mid-depth anomaly in salinity indicated the presence of dilute wastewater at Station 10. This high-precision observation demonstrated that the diffuser structure was operating better than predicted by modeling, and that the discharged wastewater experienced high levels of dilution just beyond the ZID. The amplitude of the anomaly indicates that wastewater had been diluted more than 557-fold at this location. This is four times higher than the 133:1 dilution used in the NPDES permit to establish end-of-pipe concentration limits on effluent constituents. Thus, the high dilution ratio that was determined from actual measurements during the April 2007 survey demonstrated that the outfall was performing better than expected, and that the limits on wastewater contaminant concentrations specified in the MBCSD NPDES discharge permit would easily meet the receiving-water objectives of the California Ocean Plan (COP).

NPDES Permit Limits

The seawater properties measured during the April 2007 survey were statistically evaluated for compliance with the pertinent receiving-water limitations promulgated by the NPDES discharge permit and the COP. Specifically, the permit and COP state that the discharge shall not cause the occurrence of the following conditions.

1. *Natural light to be significantly reduced at any point outside the initial dilution zone as the result of the discharge of waste*
2. *The dissolved oxygen concentration outside the zone of initial dilution to fall below 5.0 mg/L or to be depressed more than 10 percent from that which occurs naturally*
3. *The pH outside the zone of initial dilution to be depressed below 7.0, raised above 8.3, or changed more than 0.2 units from that which occurs naturally*
4. *Temperature of the receiving water to adversely affect beneficial uses*

The COP (SWRCB 1997) further defines a '*significant*' difference as '*…a statistically significant difference in the means of two distributions of sampling results at the 95 percent confidence level.*' For each observation in Tables B-1 through B-7, the statistical significance of departures from mean conditions at a given depth level were determined with an analysis of variance that compared a single observation with the mean of a larger set of samples (Sokal and Rohlf 1997, p228; Ury 1976). Although 15 independent hypothesis tests were performed at each depth level, no Bonferroni adjustment to the error

rate was included, so the tests are conservative. Specifically, Bonferroni adjustment indicates that the actual confidence level for the overall null hypothesis test for differences in properties is higher, around 99.7%, rather than the 95% level that applies to a single test. The standard deviation that was applied in the tests was determined from the entire data set to reflect the full range in ambient properties, including vertical variations.

Light Transmittance

Statistical analysis revealed significant changes in instrumentally recorded light transmittance at seven of the sixteen monitoring stations during in the April 2007 survey (highlighted by bold typeface in Table B-5). Although statistically significant, all but one of these anomalies were generated by natural fluctuations in the thickness of a turbid seafloor boundary layer that was present at all stations. As would be expected from variations in the depth of a sharply defined turbidity interface, both significant increases as well as decreases were found. Because these anomalies were generated by natural processes rather than the presence of wastewater particulates, the permit limit on natural light reductions does not apply. Even if it did, it would not apply to the three anomalies with significant increases in water clarity. Moreover, all of the anomalies were observed at depths more than twice the 6-m depth of the euphotic zone. Little natural light penetrates below the euphotic zone, so the anomalies could not have caused a "…*reduction in the transmittance of natural light.…*"

The only statistically significant discharge-related reduction in transmissivity was located at a depth of 12 m at Station 10. It constituted a localized transmissivity reduction of 13% (Table 4). Another discharge-related reduction of 5.9% was found near 9 m at Station 3, although it was not determined to be statistically significant. As with the transmissivity anomalies generated by BNL fluctuations, both of these discharge-related anomalies were too deep to materially affect the penetration of natural light. More importantly, although these two anomalies were undoubtedly related to the discharge, they were not caused by the presence of wastewater particulates. Instead, they were generated by the upward displacement of turbid bottom water that was entrained in the effluent as it was discharged near the seafloor. As such, any potential reduction in the transmission of natural light was not caused by the presence of '*waste*' particulates within the discharged effluent as specified in the COP limitation.

Dissolved Oxygen

Although it is not explicitly stated in the NPDES discharge permit, the COP specifies that the DO limitation only applies to reductions that occur "…*as a result of the discharge of oxygen demanding waste materials*." Clearly, then, the DO limitation does not apply to reductions in DO caused by the movement of ambient waters, regardless of whether or not they were induced by the physics of the discharge. This was the case for the discharge-related DO reduction observed near 9 m at Station 10 (Perturbation P2 in Table 4 and the middle frame of Figure A-7). As with the associated transmissivity anomaly, the DO anomaly was generated by the upward displacement ambient seawater that was naturally low in DO. As such, it is not subject to the permit limitation on DO reductions.

In addition, because the anomaly was created by the upward movement of ambient seawater that was naturally depleted in oxygen, the measured value was comparable to background concentrations observed elsewhere in the water column. Consequently, it would not be considered *"…depressed more than 10 percent from that which occurs naturally*." Even when compared to DO measurements at the same depth level, the amplitude of the DO anomaly (-0.53 mg/L) did not constitute a statistically significant deviation from the norm. It was also only about 5% below the average of the other DO concentrations at the same

depth level. Regardless of their origin or statistical significance, all of the 500 DO measurements were well above the 5-mg/L minimum specified in the Basin Plan and the NPDES discharge permit.

pH

None of the pH measurements were found to depart from mean conditions by more than the 95% confidence interval. This is true in the both the raw pH data (Table B-7), and in the data corrected for sensor drift (Table B-6). In addition, no pH deviations were found to spatially coincide with anomalies in other seawater properties. Spatial coincidence would suggest that they were related to the discharge. Instead, as shown in the bottom frames of Figures A-5 and A-7, the strong vertical pH gradient was laterally uniform. Regardless of their lack of statistical significance or relationship to the discharge, all of the 500 pH measurements collected during the April 2007 survey complied with the numerical limits on pH deviations in the discharge permit. All of the pH measurements remained between 7.64 and 7.90 and thus complied with the lower (7.0 pH) and upper (8.3 pH) bounds on discharge-induced pH changes. Natural oceanic processes were responsible for vertical variations in pH measurements, which were much larger than horizontal differences at a given depth level, which remained below 0.12. As such, none of the measurements can be considered changed by '*…more than 0.2 pH units from that which occurs naturally*.'

Temperature and Salinity

At -0.84ºC, the discharge-related thermal anomaly at Station 3 was too small to adversely affect beneficial uses. Moreover, as discussed previously, it was generated by the upward displacement of ambient seawater at depth. If it had, instead, been induced by the presence of dilute wastewater, it would have appeared as a positive (warmer) anomaly. In any regard, the slightly depressed temperature of 9.7ºC was comparable to average temperatures measured below the thermocline throughout the April 2007 survey. Accordingly, this thermal anomaly was not found to be statistically significant. Although this thermal anomaly was small, it compressed the thermocline at Station 3 and generated a large, artificial salinity spike.

Additionally, although salinity anomalies provide the best tracer of discharged effluent, their actual amplitude (<0.1‰) during the April 2007 survey was small compared to seasonal and spatial differences in salinity that occur along the south-central California coast. For example, differences in average salinity between the April and July surveys are typically six times higher (0.64‰). In any regard, the observed ranges in both the reported temperature (2ºC) and salinity (0.4‰) across all data collected during the April 2007 survey were too small to be considered harmful to marine biota or deleterious to beneficial uses.

Conclusions

All of the measurements recorded during the April 2007 survey complied with the receiving-water limitations specified in the NPDES discharge permit. Other than salinity and density, the discharge-related anomalies that were found near the northern ZID boundary, at Stations 3 and 10, were caused by upward displacement of ambient seawater rather than the presence of dilute effluent. At that point, effluent had been diluted at least 557-fold, and any perceptible trace of anomalous wastewater characteristics, other than low salinity, had long since disappeared. Computed dilution levels were more than four-times greater than those predicted by modeling. These measurements confirm that the diffuser structure and the outfall were operating better than expected from the modeling.

REFERENCES

California Department of Fish and Game (CDFG). 2000. Black Rockfish, *Sebastes melanops*, 1993-1999 Commercial Catch by Ports & Blocks. In: Volume 1, Marine Fisheries Profiles. California Department of Fish and Game, Marine Region. December 2000.

Davis, R.E., J.E. Dufour, G.J. Parks, and M.R. Perkins. 1982. Two Inexpensive Current-Following Drifters. Scripps Institution of Oceanography, University of California, San Diego, La Jolla, California. SIO Reference No. 82-28. December 1982.

Dohl, T.D., R.C. Guess, M.L. Duman, R.C. Helm. 1983. Cetaceans of central and northern California, 1980-1983: status, abundance, and distribution. Prepared for the U.S. the Department of the Interior, Minerals Management Service, Pacific OCS Region, Los Angeles, California. pp. 284.

Fischer, H.B., E.J. List, R.C.Y. Koh, J. Imberger, and N.H. Brooks. 1979. Mixing in Inland and Coastal Waters. New York: Academic Press, 483 p.

Herzing, D.L. and B.R. Mate. 1984. Gray whale migration along the Oregon coast, 1978-1981. In: M.L. Jones, S.L. Swartz, and S. Leatherwood [Eds.]. The Gray Whale, *Eschrichtius robustus*. Academic Press: Orlando, Florida. pp. 289-307.

Kuehl, S.A., C.A. Nittrouer, M.A. Allison, L. Ercilio, C. Faria, D.A. Dukat, J.M. Jaeger, T.D. Pacioni, A.G. Figueiredo, and E.C. Underkoffler 1996. Sediment deposition, accumulation, and seabed dynamics in an energetic fine-grained coastal environment. *Continental Shelf Research*, 16: 787-816.

Marine Research Specialists (MRS). 1998a. City of Morro Bay and Cayucos Sanitary District, Offshore Monitoring and Reporting Program, Water Column Sampling, March 1998 Survey. Prepared for the City of Morro Bay, CA. April 1998.

Marine Research Specialists (MRS). 1998b. City of Morro Bay and Cayucos Sanitary District, Offshore Monitoring and Reporting Program, Semiannual Benthic Sampling Report, April 1998 Survey. Prepared for the City of Morro Bay, CA. July 1998.

Marine Research Specialists (MRS). 1998c. City of Morro Bay and Cayucos Sanitary District, Offshore Monitoring and Reporting Program, Water Column Sampling, July 1998 Survey. Prepared for the City of Morro Bay, CA. August 1998.

Marine Research Specialists (MRS). 2000. City of Morro Bay and Cayucos Sanitary District, Offshore Monitoring and Reporting Program, 1999 Annual Report. Prepared for the City of Morro Bay, California. February 2000.

Marine Research Specialists (MRS). 2001. City of Morro Bay and Cayucos Sanitary District, Offshore Monitoring and Reporting Program, 2000 Annual Report. Prepared for the City of Morro Bay, California. February 2001.

Marine Research Specialists (MRS). 2002. City of Morro Bay and Cayucos Sanitary District, Offshore Monitoring and Reporting Program, 2001 Annual Report. Prepared for the City of Morro Bay, California. February 2002.

Marine Research Specialists (MRS). 2003. City of Morro Bay and Cayucos Sanitary District, Offshore Monitoring and Reporting Program, 2002 Annual Report. Prepared for the City of Morro Bay, California. February 2003.

Marine Research Specialists (MRS). 2004. City of Morro Bay and Cayucos Sanitary District, Offshore Monitoring and Reporting Program, 2003 Annual Report. Prepared for the City of Morro Bay, California. February 2004.

Marine Research Specialists (MRS). 2005. City of Morro Bay and Cayucos Sanitary District, Offshore Monitoring and Reporting Program, 2004 Annual Report. Prepared for the City of Morro Bay, California. February 2005.

Marine Research Specialists (MRS). 2006. City of Morro Bay and Cayucos Sanitary District, Offshore Monitoring and Reporting Program, 2005 Annual Report. Prepared for the City of Morro Bay, California. February 2006.

Marine Research Specialists (MRS). 2007. City of Morro Bay and Cayucos Sanitary District, Offshore Monitoring and Reporting Program, 2006 Annual Report. Prepared for the City of Morro Bay, California. February 2007.

Morro Group, Inc. 2000. MFS Globenet Corp./WorldCom Network Services Fiber Optic Cable Project Final Environmental Impact Report. SCH No. 98091053. Volume I. Submitted to: County of San Luis Obispo Department of Planning and Building. Prepared in association with Arthur D. Little, Inc. and Marine Research Specialists. January 2000.

Regional Water Quality Control Board (RWQCB) - Central Coast Region. 1994. Water Quality Control Plan (Basin Plan) Central Coast Region. Available from the RWQCB at 81 Higuera Street, Suite 200, San Luis Obispo, California. 148p. + Appendices.

Regional Water Quality Control Board (RWQCB) - Central Coast Region. 1998. Administrative Extension of Waste Discharge Requirements/National Pollution Discharge Elimination System (NPDES) CA0047881, Order 92-67. Letter to Mr. William Boucher, Director of Public Works, City of Morro Bay from Roger W. Briggs, Executive Officer. 10 April 1998.

Regional Water Quality Control Board (RWQCB) - Central Coast Region and the Environmental Protection Agency (EPA) – Region IX. 1998a. Waste Discharge Requirements (Order No. 98-15) and National Pollutant Discharge Elimination System (Permit No. CA0047881) for City of Morro bay and Cayucos Sanitary District, San Luis Obispo County. 11 December 1998.

Regional Water Quality Control Board (RWQCB) - Central Coast Region and the Environmental Protection Agency (EPA) – Region IX. 1998b. Monitoring and Reporting Program No. 98-15 for City of Morro Bay and Cayucos Sanitary District, San Luis Obispo County. 11 December 1998.

Reilly, S.B. 1984. Assessing gray whale abundance: a review. In: M.L. Jones, S.L. Swartz, and S. Leatherwood [Eds.]. The Gray Whale, *Eschrichtius robustus*. Orlando, Florida: Academic Press. pp. 203-223.

Rice, D.W., A.A. Wolman and H.W. Braham. 1984. The gray whale, *Eschrichtius robustus*. In: J.M. Briewick and H.W. Braham [Eds.]. The Status of Endangered Whales. Mar. Fish. Rev. 46(4):7-14.

Rugh, D.J. 1984. Census of gray whales at Unimak Pass, Alaska: November-December 1977-1979. In: M.L. Jones, S.L. Swartz, and S. Leatherwood. (Eds.). The Gray Whale, *Eschrichtius robustus*. Orlando, Florida: Academic Press. pp. 225-248.

Sea-Bird Electronics, Inc. (SBE) 1989. Calculation of M and B Coefficients for the Sea-Tech Transmissometer. Application Note No. 7, Revised September 1989.

Sea-Bird Electronics, Inc. (SBE) 1993. SBE 13/22/23/30 Dissolved Oxygen Sensor Calibration and Deployment. Application Note No. 13-1, rev B, Revised April 1993.

Sokal, R.R. and F.J. Rohlf. 1997. Biometry: the Principals and Practice of Statistics in Biological Research, 3rd ed. New York: W.H. Freeman and Company, 850 p.

Southern California Bight Pilot Project Field Coordination Team (SCBPPFCT). 1995. Field Operation Manual for Marine Water-Column, Benthic, and Trawl monitoring in Southern California. August 22, 1995.

State Water Resources Control Board (SWRCB). 1997. Water quality control plan, ocean waters of California, California Ocean Plan. California Environmental Protection Agency. Effective July 23, 1997.

Sund, P.N. and J.L. O'Connor. 1974. Aerial observations of gray whales during 1973. Mar. Fish. Rev. 36(4):51-55.

Tetra Tech. 1992. Technical Review City of Morro Bay, CA Section 301(h) Application for Modification of Secondary Treatment Requirements for a Discharge into Marine Waters. Prepared for the U.S. Environmental Protection Agency, Region IX, San Francisco, CA by Tetra Tech, Inc., Lafayette, CA. February 1992.

Ury, H.K. 1976. A comparison of four procedures for multiple comparisons among means (pairwise contrasts) for arbitrary sample sizes. *Technometrics*, 18: 89–97.

APPENDIX A

Water Quality Profiles and Cross Sections

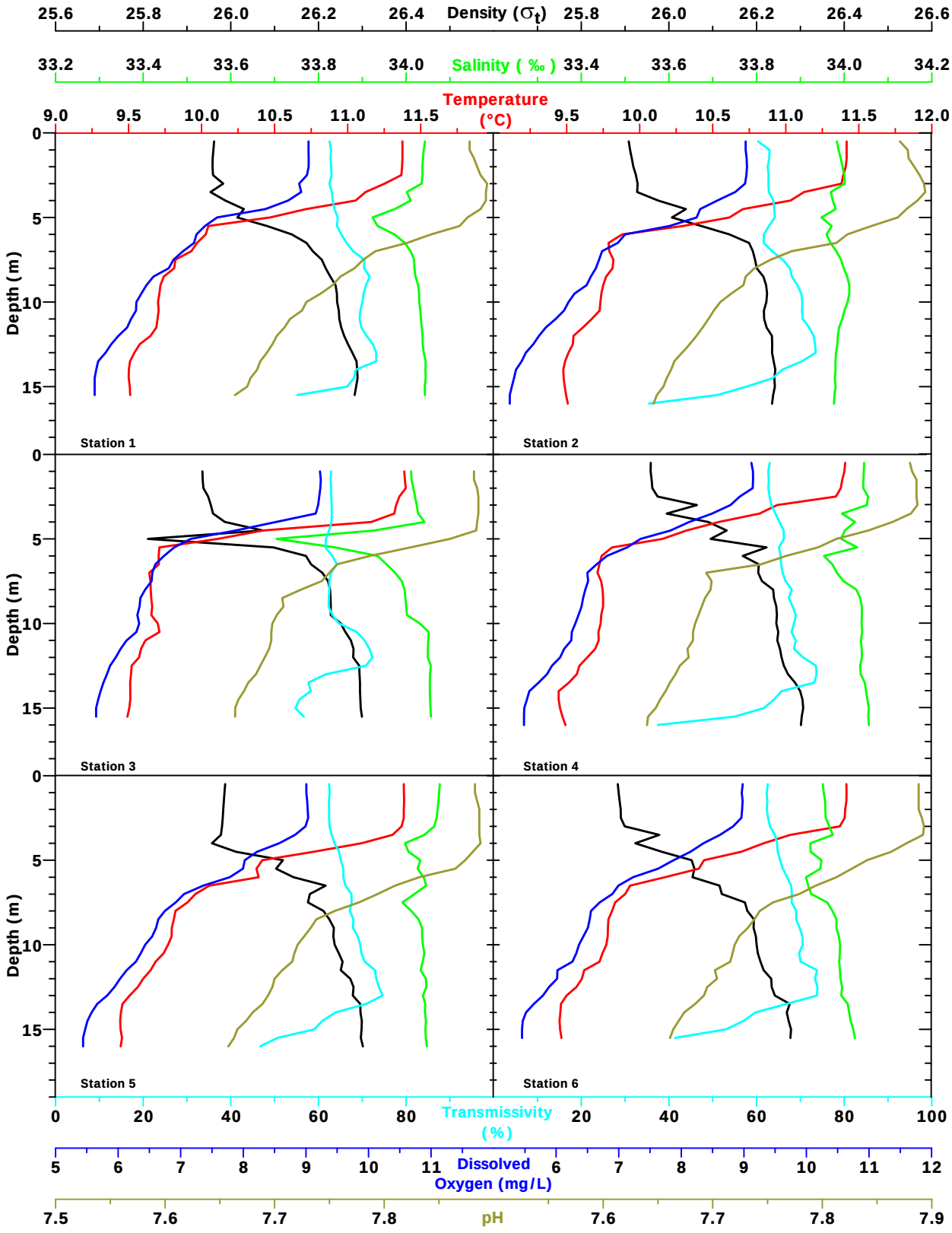

Figure A-1. Vertical Profiles of Water-Quality Parameters for Stations 1 through 6 measured on 28 April 2007

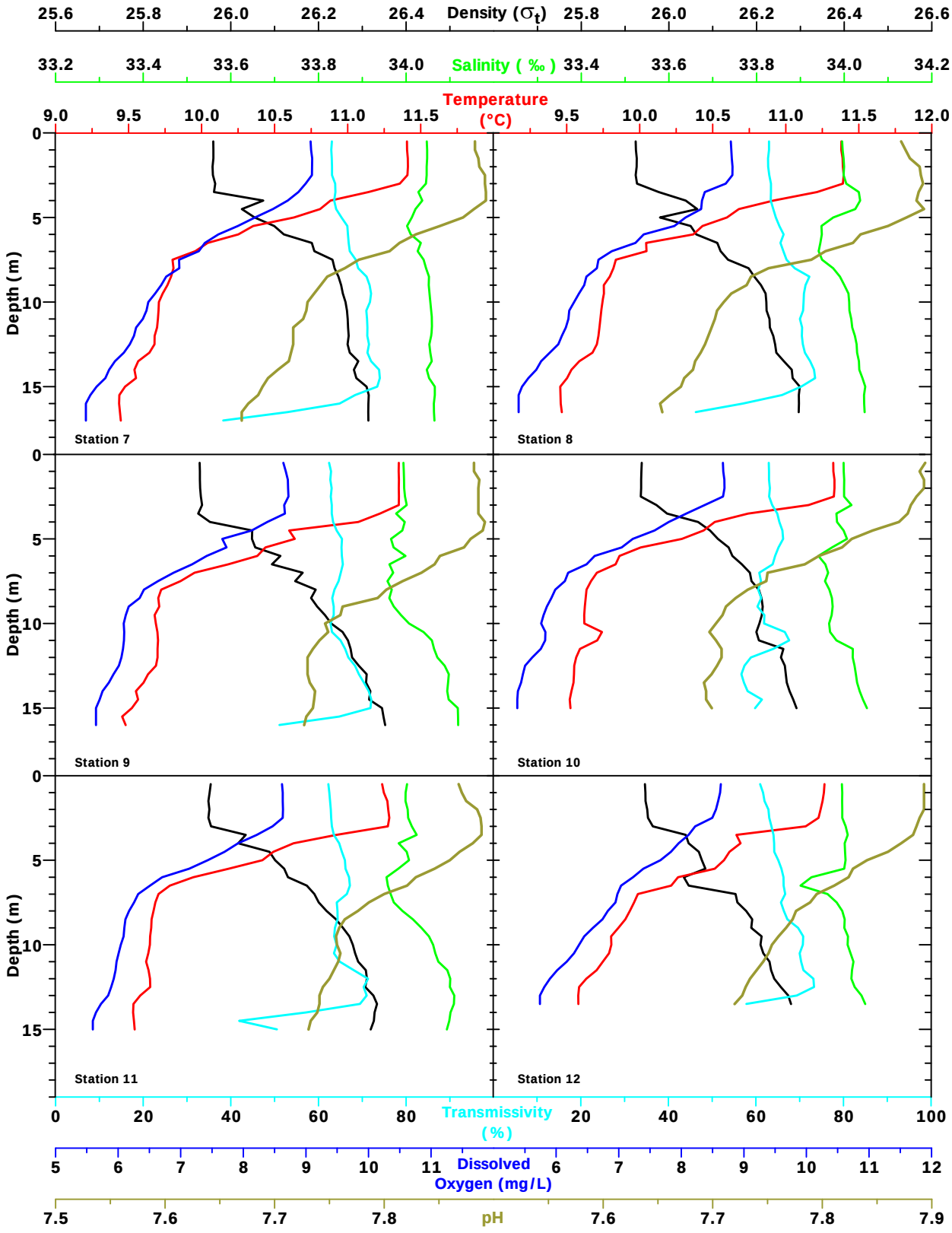

Figure A-2. Vertical Profiles of Water-Quality Parameters for Stations 7 through 12 measured on 28 April 2007

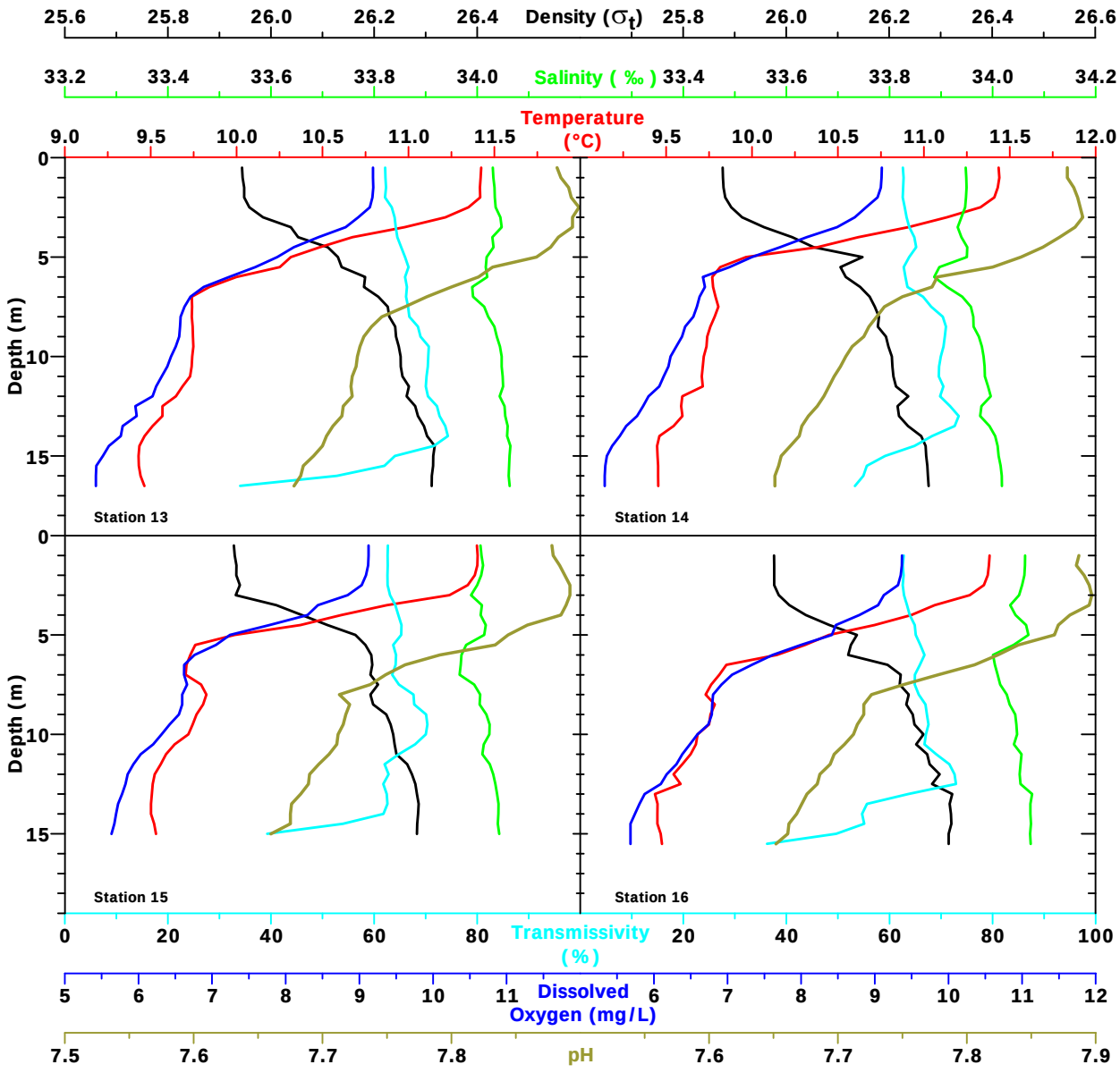

Figure A-3. Vertical Profiles of Water-Quality Parameters for Stations 13 through 16 measured on 28 April 2007

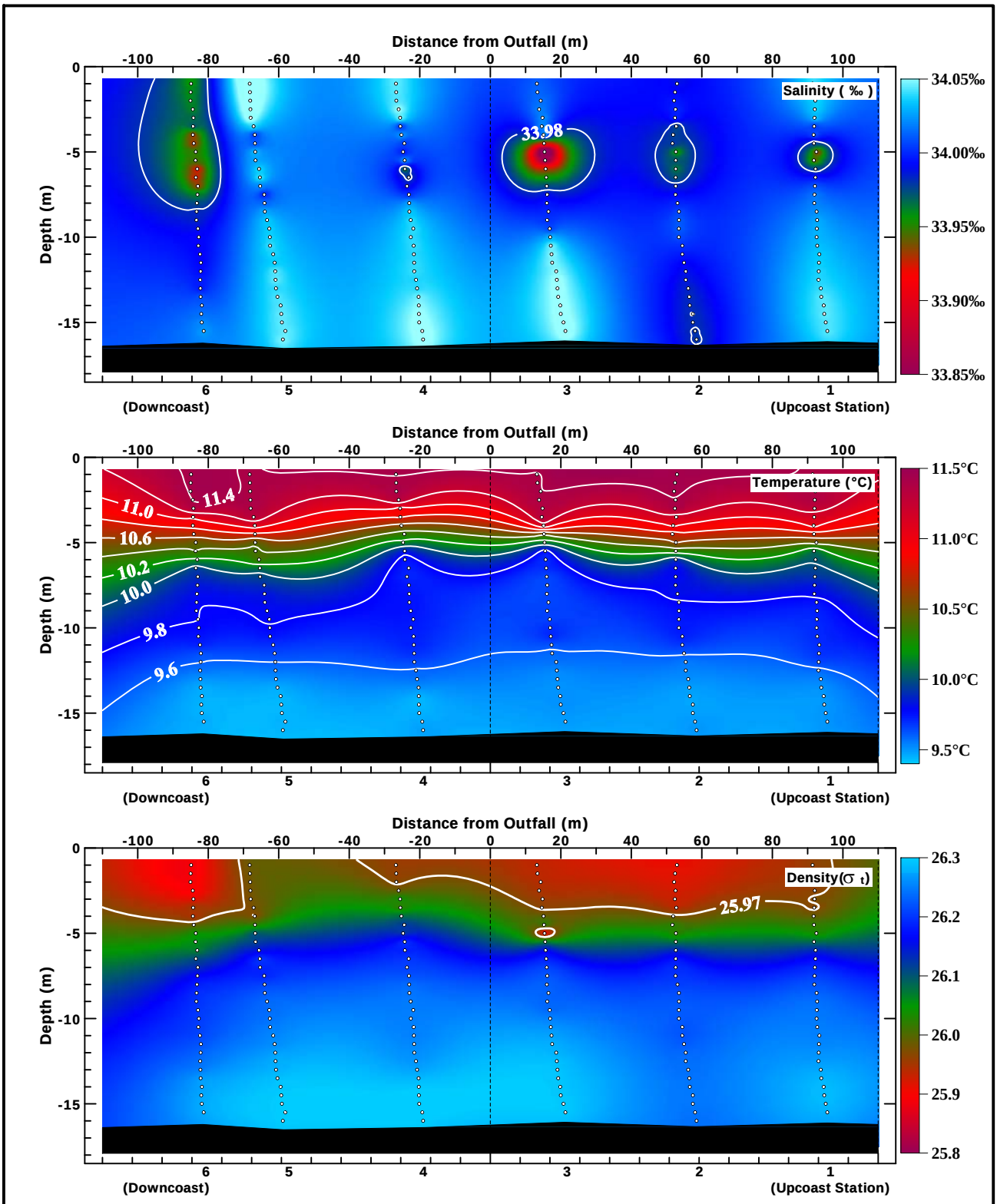

Figure A-4. Along-Shore Transects of Salinity, Temperature, and Density on 28 April 2007

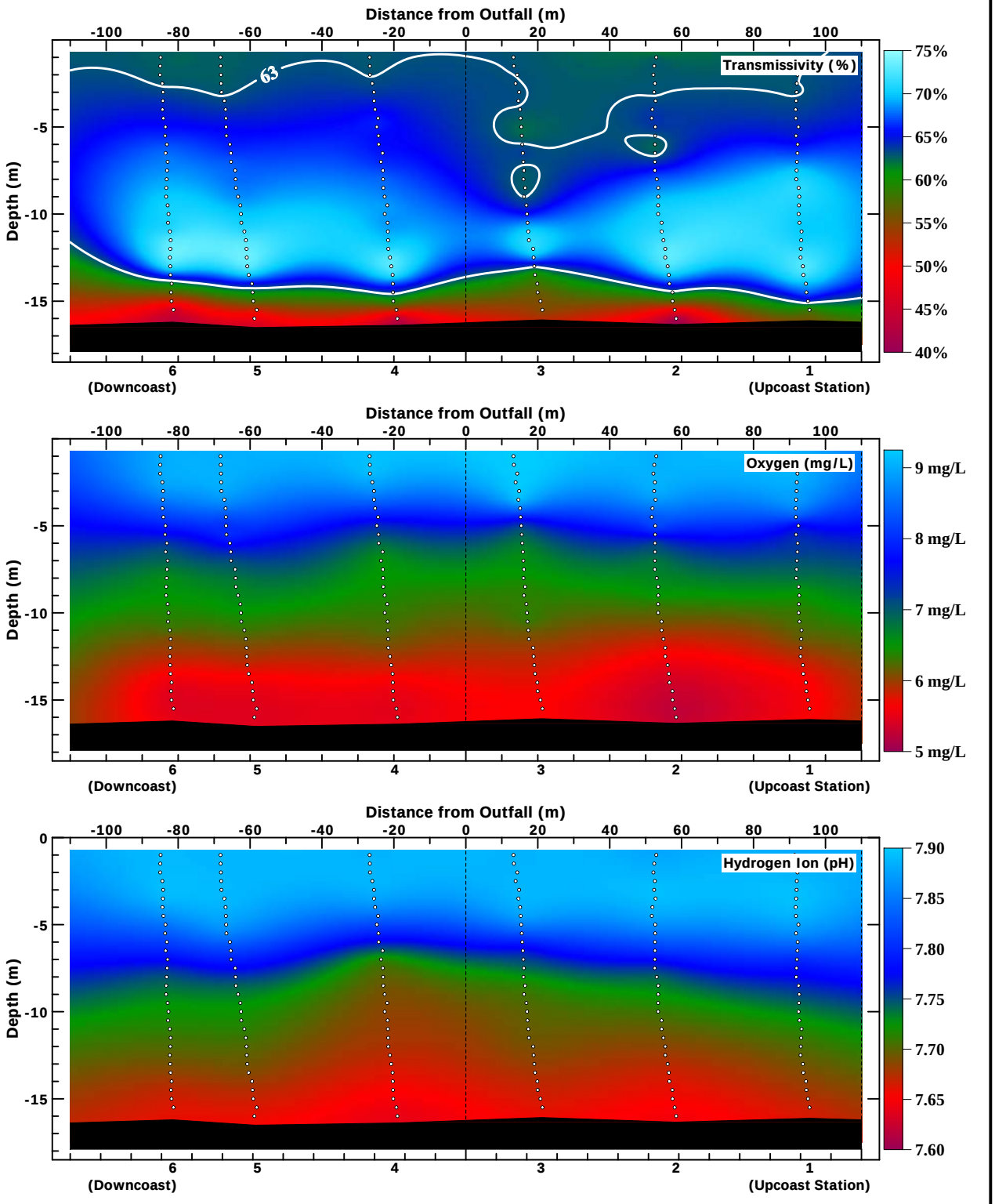

Figure A-5. Along-Shore Transects of Transmissivity, Oxygen, and pH on 28 April 2007

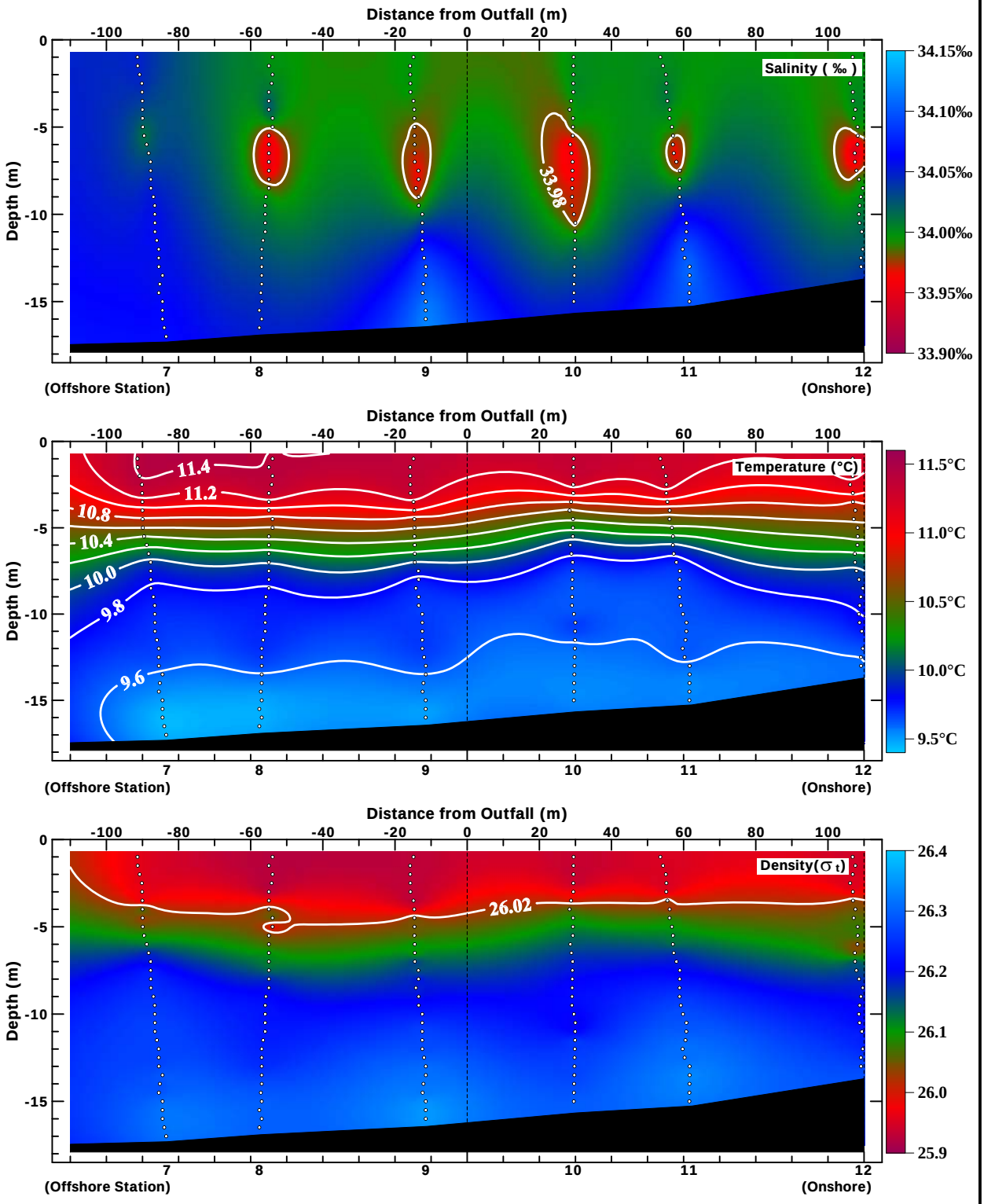

Figure A-6. Cross-Shore Transects of Salinity, Temperature, and Density on 28 April 2007

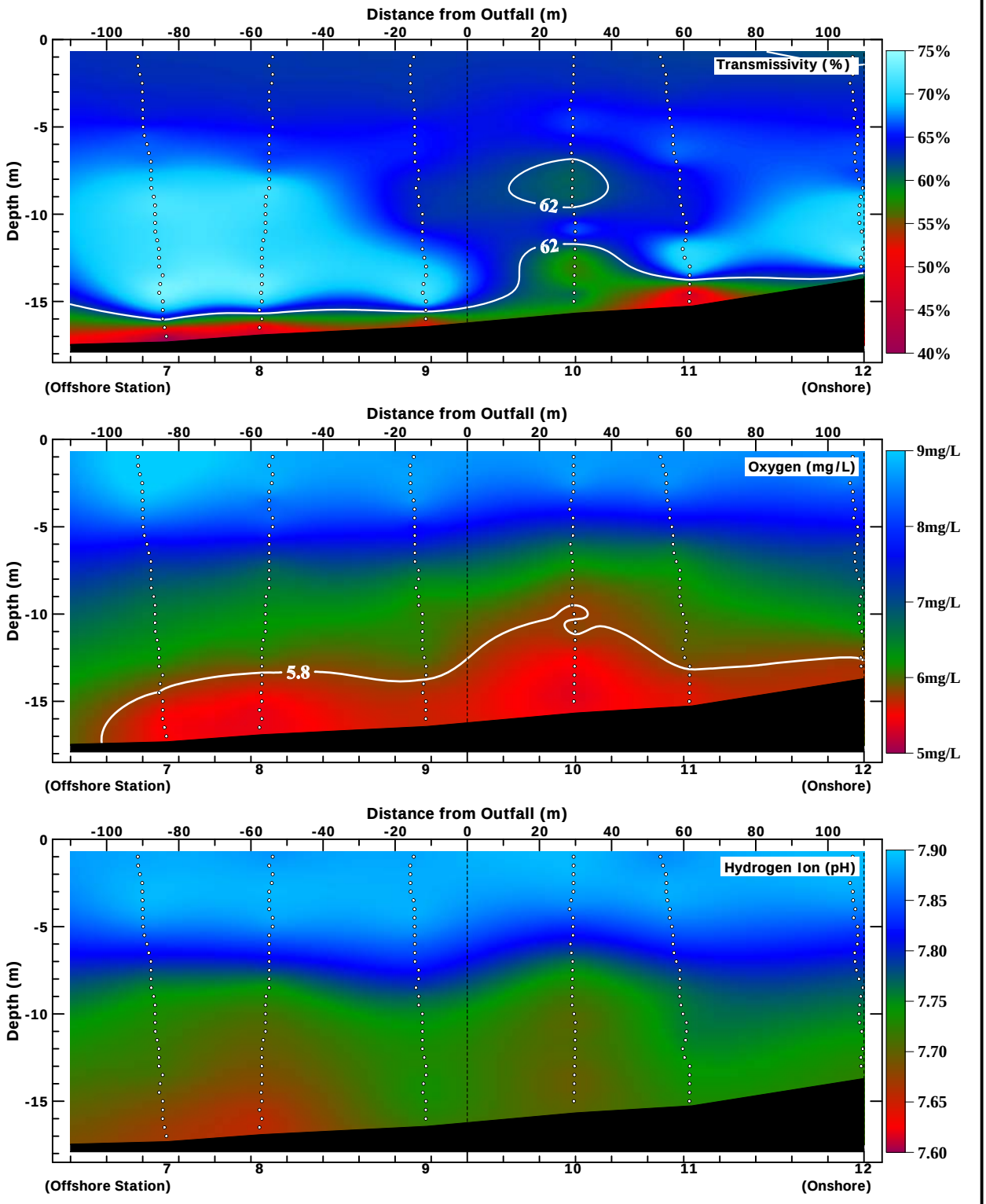

Figure A-7. Cross-Shore Transects of Transmissivity, Oxygen, and pH on 28 April 2007

APPENDIX B

Tables of Profile Data and Standard Observations

Table B-1. Seawater Temperature on 28 April 2007

	Temperature (°C)															
Depth (m)	**1**	**2**	**3**	**4**	**5**	**6**	**7**	**8**	**9**	**10**	**11**	**12**	**13**	**14**	**15**	**16**
0.5	11.38	11.42		11.41	11.38	11.42	11.41	11.38	11.35	11.33	11.24	11.27	11.42	11.44	11.40	
1.0	11.38	11.42	11.39	11.40	11.39	11.42	11.41	11.38	11.35	11.33	11.25	11.26	11.42	11.44	11.40	11.38
1.5	11.38	11.42	11.39	11.39	11.39	11.42	11.41	11.39	11.35	11.33	11.27	11.25	11.42	11.43	11.40	11.38
2.0	11.37	11.41	11.40	11.38	11.38	11.41	11.41	11.39	11.35	11.33	11.28	11.24	11.42	11.41	11.39	11.37
2.5	11.37	11.39	11.35	11.34	11.38	11.40	11.41	11.40	11.35	11.33	11.29	11.22	11.35	11.33	11.34	11.35
3.0	11.25	11.38	11.33	10.94	11.37	11.37	11.36	11.39	11.35	11.16	11.28	11.14	11.22	11.13	11.24	11.27
3.5	11.12	11.13	11.32	10.82	11.31	11.03	11.14	11.21	11.22	10.74	10.92	10.66	10.98	10.91	10.87	11.06
4.0	11.05	11.03	11.16	10.54	11.09	10.85	10.88	10.92	11.07	10.51	10.63	10.69	10.67	10.62	10.61	10.93
4.5	10.72	10.71	10.42	10.32	10.77	10.69	10.81	10.68	10.60	10.44	10.49	10.61	10.48	10.38	10.37	10.71
5.0	10.47	10.61	10.11	10.16	10.42	10.44	10.63	10.60	10.64	10.29	10.42	10.58	10.32	9.96	9.99	10.45
5.5	10.05	10.30	9.71	9.81	10.38	10.40	10.35	10.43	10.44	10.01	10.19	10.51	10.25	9.82	9.76	10.31
6.0	10.03	9.88	9.71	9.74	10.39	10.17	10.25	10.37	10.38	9.86	9.94	10.26	10.00	9.77	9.73	10.14
6.5	9.97	9.79	9.71	9.72	10.05	9.93	10.04	10.04	10.18	9.83	9.78	10.22	9.84	9.77	9.71	9.85
7.0	9.93	9.79	9.64	9.71	9.96	9.90	9.96	10.05	9.95	9.71	9.71	9.99	9.74	9.79	9.70	9.81
7.5	9.82	9.82	9.65	9.74	9.90	9.83	9.80	9.84	9.86	9.67	9.68	9.96	9.74	9.80	9.79	9.76
8.0	9.81	9.81	9.65	9.75	9.82	9.81	9.81	9.82	9.72	9.64	9.67	9.93	9.74	9.78	9.82	9.73
8.5	9.74	9.77	9.65	9.75	9.81	9.79	9.79	9.79	9.70	9.63	9.66	9.90	9.74	9.76	9.81	9.78
9.0	9.72	9.75	9.66	9.75	9.80	9.78	9.77	9.75	9.71	9.62	9.65	9.85	9.75	9.74	9.77	9.76
9.5	9.71	9.74	9.66	9.74	9.79	9.78	9.73	9.75	9.68	9.62	9.65	9.80	9.75	9.73	9.74	9.75
10.0	9.70	9.73	9.70	9.73	9.77	9.77	9.71	9.75	9.69	9.62	9.65	9.81	9.74	9.72	9.72	9.68
10.5	9.71	9.73	9.71	9.72	9.74	9.74	9.70	9.74	9.70	9.74	9.63	9.79	9.74	9.71	9.64	9.67
11.0	9.70	9.67	9.61	9.72	9.68	9.72	9.70	9.73	9.70	9.71	9.62	9.75	9.73	9.71	9.59	9.64
11.5	9.69	9.61	9.59	9.69	9.65	9.62	9.69	9.73	9.70	9.59	9.64	9.70	9.68	9.71	9.56	9.59
12.0	9.65	9.55	9.57	9.64	9.60	9.60	9.68	9.72	9.70	9.57	9.65	9.63	9.65	9.59	9.52	9.54
12.5	9.58	9.54	9.52	9.59	9.56	9.57	9.68	9.71	9.69	9.55	9.65	9.59	9.57	9.59	9.51	9.58
13.0	9.54	9.51	9.52	9.57	9.51	9.50	9.64	9.68	9.63	9.55	9.58	9.58	9.57	9.59	9.51	9.43
13.5	9.51	9.49	9.51	9.51	9.46	9.46	9.57	9.59	9.60	9.55	9.53	9.58	9.51	9.54	9.50	9.45
14.0	9.50	9.48	9.51	9.45	9.45	9.46	9.54	9.53	9.55	9.53	9.53		9.46	9.46	9.50	9.45
14.5	9.50	9.48	9.51	9.44	9.44	9.45	9.55	9.50	9.56	9.52	9.54		9.43	9.45	9.52	9.45
15.0	9.51	9.49	9.50	9.45	9.44	9.45	9.48	9.46	9.52	9.53	9.54		9.43	9.45	9.53	9.47
15.5	9.51	9.50	9.49	9.47	9.45	9.46	9.44	9.46	9.46				9.43	9.45		9.48
16.0		9.51		9.49	9.45		9.43	9.46	9.48				9.44	9.45		
16.5							9.44	9.47					9.46	9.45		
17.0							9.45									

Table B-2. Salinity[1] on 28 April 2007

	Salinity (‰)															
Depth (m)	**1**	**2**	**3**	**4**	**5**	**6**	**7**	**8**	**9**	**10**	**11**	**12**	**13**	**14**	**15**	**16**
0.5	34.043	33.983		34.046	34.077	33.951	34.047	33.995	33.994	33.999	34.002	33.995	34.030	33.948	34.006	
1.0	34.040	33.987	34.011	34.045	34.075	33.953	34.048	33.996	33.995	33.999	33.999	33.996	34.031	33.949	34.008	34.063
1.5	34.039	33.992	34.013	34.044	34.074	33.956	34.048	33.999	33.995	34.000	33.999	33.995	34.034	33.949	34.011	34.063
2.0	34.037	33.996	34.017	34.044	34.072	33.957	34.047	34.000	33.996	34.000	34.004	33.996	34.034	33.948	34.008	34.062
2.5	34.038	34.000	34.021	34.054	34.070	33.958	34.047	33.999	33.998	34.000	34.005	33.996	34.036	33.947	34.000	34.057
3.0	34.035	34.001	34.024	34.052	34.065	33.966	34.045	34.005	34.001	34.017	34.013	34.003	34.045	33.940	33.988	34.051
3.5	34.002	33.969	34.028	33.995	34.042	33.974	34.028	34.034	33.977	33.982	34.024	34.008	34.047	33.932	34.009	34.034
4.0	34.011	33.974	34.042	34.025	33.998	**33.923**	34.037	34.037	33.997	33.984	33.983	34.001	34.029	33.940	34.007	34.045
4.5	33.975	33.981	33.927	34.001	34.006	33.924	34.021	34.026	33.992	33.999	34.001	34.002	34.032	33.951	34.017	34.065
5.0	33.923	33.948	**33.705**	33.993	34.033	33.948	34.013	33.975	33.966	34.006	34.007	34.003	34.018	33.950	34.014	***34.069***
5.5	33.935	33.972	**33.838**	34.030	34.026	33.946	34.002	33.948	33.971	33.972	33.983	34.000	34.017	33.897	33.979	34.041
6.0	33.973	33.960	33.935	33.954	34.040	33.913	34.011	33.949	33.999	33.941	33.955	33.926	34.019	33.887	33.970	34.001
6.5	33.997	33.969	33.955	33.973	34.046	33.918	34.034	33.946	33.962	33.957	33.958	33.901	33.990	33.912	33.968	34.004
7.0	34.010	33.982	33.975	33.983	34.019	33.925	34.026	33.942	33.971	33.963	33.965	33.962	33.992	33.941	33.966	34.010
7.5	34.018	33.993	33.990	33.998	33.992	33.961	34.040	33.949	33.958	33.956	33.972	33.983	34.014	33.958	33.994	34.015
8.0	34.019	33.999	33.997	34.028	34.012	33.973	34.046	33.975	33.967	33.966	33.992	33.996	34.021	33.962	34.006	34.027
8.5	34.022	34.007	33.999	34.036	34.029	33.982	34.053	33.991	33.962	33.972	34.016	34.001	34.033	33.963	34.005	34.033
9.0	34.028	34.012	34.000	34.040	34.036	33.983	34.052	34.001	33.972	33.974	34.035	34.000	34.038	33.973	34.018	34.044
9.5	34.030	34.012	34.002	34.041	34.037	33.988	34.053	34.010	33.988	33.971	34.052	34.009	34.044	33.979	34.024	34.046
10.0	34.030	34.008	34.032	34.040	34.038	33.991	34.056	34.011	34.007	33.966	34.062	34.008	34.048	33.982	34.024	34.048
10.5	34.033	34.001	34.051	34.041	34.042	33.990	34.058	34.012	34.040	33.968	34.067	34.014	34.047	33.984	34.013	34.041
11.0	34.034	33.996	34.051	34.038	34.038	33.989	34.059	34.016	34.059	33.982	34.074	34.021	34.049	33.985	34.010	34.056
11.5	34.036	33.988	34.050	34.040	34.033	33.991	34.059	34.018	34.064	34.020	34.094	34.018	34.051	33.991	34.024	34.054
12.0	34.038	33.986	34.050	34.041	34.046	33.992	34.057	34.025	34.071	34.019	34.101	34.017	34.044	33.997	34.031	34.052
12.5	34.038	33.984	34.056	34.036	34.046	33.995	34.053	34.029	34.088	34.024	34.100	34.024	34.053	33.978	34.035	34.054
13.0	34.040	33.981	34.055	34.038	34.039	33.993	34.055	34.029	34.098	34.027	34.110	34.040	34.054	33.976	34.039	34.077
13.5	34.045	33.980	34.054	34.047	34.044	34.008	34.059	34.034	34.096	34.029	34.109	34.048	34.059	33.994	34.042	34.073
14.0	34.044	33.980	34.054	34.050	34.043	34.011	34.047	34.034	34.094	34.035	34.101		34.058	34.005	34.041	34.073
14.5	34.045	33.979	34.055	34.053	34.045	34.015	34.053	34.042	34.097	34.043	34.099		34.065	34.010	34.040	34.074
15.0	34.043	33.980	34.056	34.056	34.045	34.021	34.066	34.048	34.118	34.052	34.093		34.063	34.012	34.043	34.073
15.5	34.043	33.978	34.057	34.055	34.045	34.024	34.066	34.045	34.119				34.062	34.015		34.074
16.0		33.977		34.057	34.048		34.063	34.046	34.119				34.061	34.018		
16.5							34.064	34.047					34.063	34.018		
17.0							34.065									

[1] Values enclosed in boxes differed significantly from the mean of other salinity measurements at the same distance below the sea surface.
The thinner boxes encompass values that were significantly higher than the mean of other measurements at the same distance below the sea surface.

Table B-3. Seawater Density on 28 April 2007

	Density (sigma-t)															
Depth (m)	**1**	**2**	**3**	**4**	**5**	**6**	**7**	**8**	**9**	**10**	**11**	**12**	**13**	**14**	**15**	**16**
0.5	25.962	25.908		25.959	25.987	25.883	25.960	25.924	25.929	25.938	25.954	25.945	25.944	25.877	25.928	
1.0	25.960	25.911	25.935	25.958	25.985	25.885	25.960	25.925	25.929	25.937	25.952	25.946	25.945	25.877	25.930	25.976
1.5	25.959	25.915	25.936	25.960	25.984	25.887	25.960	25.927	25.930	25.937	25.949	25.947	25.948	25.878	25.933	25.977
2.0	25.958	25.919	25.938	25.962	25.983	25.890	25.958	25.926	25.930	25.937	25.951	25.951	25.948	25.882	25.933	25.977
2.5	25.960	25.925	25.948	25.974	25.982	25.890	25.959	25.924	25.932	25.936	25.949	25.952	25.958	25.894	25.940	25.977
3.0	25.983	25.928	25.954	26.064	25.980	25.899	25.965	25.927	25.934	25.971	25.955	25.963	25.984	25.914	25.932	25.986
3.5	25.954	25.928	25.960	25.995	25.978	25.978	25.962	25.976	25.926	25.996	26.034	26.038	26.039	25.957	26.011	26.006
4.0	25.988	25.976	25.987	26.090	25.957	25.923	26.074	26.038	25.952	26.066	26.017	26.045	26.053	26.012	26.060	26.038
4.5	26.030	26.039	26.073	26.132	26.012	25.984	26.025	26.064	26.049	26.094	26.088	26.068	26.110	26.053	26.110	26.084
5.0	26.015	26.007	**25.811**	26.095	26.119	26.052	26.054	25.980	26.048	26.112	26.101	26.075	26.130	26.148	26.164	26.138
5.5	26.083	26.074	26.097	26.223	26.103	26.058	26.099	26.050	26.056	26.136	26.122	26.083	26.137	26.105	26.183	26.126
6.0	26.139	26.138	26.172	26.169	26.143	26.054	26.121	26.062	26.113	26.145	26.131	26.034	26.182	26.116	26.195	26.121
6.5	26.173	26.183	26.183	26.205	26.216	26.115	26.185	26.111	26.094	26.166	26.174	26.045	26.180	26.144	26.196	26.197
7.0	26.187	26.192	26.209	26.204	26.180	26.121	26.191	26.118	26.164	26.185	26.191	26.152	26.208	26.162	26.193	26.222
7.5	26.208	26.197	26.222	26.212	26.176	26.173	26.232	26.135	26.147	26.189	26.201	26.156	26.226	26.172	26.207	26.220
8.0	26.217	26.200	26.227	26.238	26.212	26.179	26.237	26.182	26.194	26.205	26.219	26.176	26.229	26.180	26.193	26.238
8.5	26.227	26.216	26.228	26.240	26.225	26.194	26.246	26.195	26.183	26.211	26.240	26.190	26.241	26.178	26.198	26.233
9.0	26.239	26.222	26.228	26.245	26.235	26.193	26.252	26.210	26.197	26.214	26.256	26.188	26.243	26.194	26.224	26.246
9.5	26.242	26.224	26.228	26.247	26.234	26.198	26.256	26.221	26.215	26.212	26.271	26.212	26.248	26.199	26.232	26.249
10.0	26.243	26.223	26.251	26.245	26.237	26.200	26.262	26.222	26.229	26.206	26.278	26.209	26.251	26.205	26.237	26.267
10.5	26.247	26.217	26.261	26.249	26.246	26.203	26.265	26.223	26.255	26.200	26.284	26.215	26.252	26.206	26.240	26.253
11.0	26.248	26.218	26.274	26.247	26.255	26.209	26.267	26.230	26.268	26.205	26.291	26.230	26.255	26.208	26.244	26.274
11.5	26.252	26.223	26.280	26.254	26.251	26.216	26.268	26.230	26.274	26.261	26.31	26.233	26.268	26.213	26.264	26.278
12.0	26.259	26.235	26.279	26.257	26.273	26.233	26.269	26.238	26.277	26.256	26.311	26.240	26.263	26.237	26.273	26.298
12.5	26.268	26.236	26.293	26.262	26.280	26.235	26.266	26.242	26.292	26.265	26.307	26.255	26.280	26.216	26.280	26.283
13.0	26.277	26.235	26.294	26.272	26.278	26.242	26.272	26.245	26.310	26.267	26.325	26.272	26.285	26.219	26.283	26.322
13.5	26.287	26.239	26.295	26.288	26.295	26.276	26.291	26.263	26.309	26.269	26.334	26.279	26.297	26.237	26.287	26.318
14.0	26.288	26.243	26.295	26.299	26.296	26.269	26.281	26.280	26.318	26.275	26.328		26.303	26.262	26.286	26.320
14.5	26.290	26.241	26.296	26.305	26.299	26.273	26.287	26.282	26.316	26.284	26.326		26.317	26.271	26.284	26.321
15.0	26.286	26.242	26.296	26.306	26.299	26.279	26.310	26.299	26.345	26.291	26.319		26.315	26.272	26.283	26.316
15.5	26.283	26.238	26.300	26.303	26.297	26.278	26.315	26.296	26.348				26.314	26.274		26.316
16.0		26.236		26.301	26.301		26.314	26.297	26.353				26.312	26.275		
16.5							26.314	26.296					26.312	26.277		
17.0							26.314									

[1] Values enclosed in boxes were significantly lower than the mean of other density measurements at the same distance below the sea surface.

Table B-4. Dissolved Oxygen on 28 April 2007

	Dissolved Oxygen (mg/L)															
Depth (m)	**1**	**2**	**3**	**4**	**5**	**6**	**7**	**8**	**9**	**10**	**11**	**12**	**13**	**14**	**15**	**16**
0.5	9.04	9.03		9.12	9.01	8.98	9.07	8.79	8.64	8.67	8.62	8.63	9.19	9.10	9.12	
1.0	9.04	9.03	9.22	9.15	9.01	8.97	9.08	8.80	8.68	8.67	8.63	8.62	9.19	9.09	9.12	9.37
1.5	9.04	9.05	9.24	9.15	9.02	8.98	9.10	8.81	8.71	8.69	8.63	8.59	9.19	9.08	9.12	9.37
2.0	9.04	9.05	9.23	9.14	9.03	8.97	9.10	8.82	8.72	8.69	8.63	8.55	9.18	9.04	9.09	9.35
2.5	9.02	9.04	9.21	8.93	9.03	8.96	9.10	8.82	8.72	8.67	8.63	8.50	9.14	8.88	9.03	9.32
3.0	8.89	9.02	9.20	8.79	8.99	8.83	8.99	8.71	8.65	8.37	8.47	8.22	8.98	8.73	8.84	9.12
3.5	8.93	8.86	9.16	8.49	8.82	8.62	8.88	8.38	8.67	8.08	8.22	8.12	8.81	8.49	8.43	9.04
4.0	8.72	8.58	8.52	8.13	8.57	8.35	8.71	8.33	8.38	7.80	7.92	7.96	8.44	8.07	8.30	8.79
4.5	8.35	8.30	7.88	7.83	8.22	8.15	8.47	8.32	8.13	7.57	7.70	7.83	8.11	7.71	7.78	8.47
5.0	7.58	8.24	7.16	7.35	8.02	7.88	8.19	8.07	7.66	7.23	7.43	7.67	7.89	7.33	7.24	8.42
5.5	7.39	7.81	6.90	7.13	8.00	7.63	7.91	7.89	7.73	7.05	7.13	7.39	7.59	7.03	7.05	8.00
6.0	7.25	7.10	6.73	6.81	7.78	7.23	7.60	7.40	7.41	6.62	6.70	7.23	7.23	6.67	6.76	7.61
6.5	7.21	6.98	6.59	6.65	7.36	6.99	7.39	7.27	7.18	6.48	6.51	7.04	6.88	6.69	6.62	7.33
7.0	7.04	6.73	6.55	6.50	7.05	6.90	7.29	6.89	6.89	6.19	6.32	6.98	6.71	6.62	6.62	7.06
7.5	6.89	6.69	6.54	6.51	6.92	6.69	6.97	6.68	6.64	6.14	6.25	6.95	6.63	6.58	6.66	6.92
8.0	6.81	6.63	6.43	6.47	6.75	6.56	6.98	6.65	6.41	5.99	6.18	6.83	6.57	6.53	6.59	6.80
8.5	6.56	6.55	6.35	6.43	6.64	6.54	6.77	6.48	6.34	5.92	6.12	6.74	6.57	6.42	6.59	6.79
9.0	6.45	6.49	6.34	6.40	6.61	6.51	6.69	6.45	6.17	5.85	6.10	6.59	6.55	6.38	6.55	6.79
9.5	6.37	6.29	6.31	6.36	6.55	6.43	6.59	6.36	6.12	5.80	6.09	6.45	6.51	6.30	6.42	6.74
10.0	6.29	6.20	6.34	6.30	6.43	6.36	6.48	6.29	6.09	5.76	6.04	6.37	6.44	6.23	6.31	6.59
10.5	6.29	6.13	6.29	6.25	6.36	6.32	6.45	6.21	6.10	5.83	6.01	6.28	6.39	6.20	6.20	6.49
11.0	6.21	5.99	6.14	6.24	6.28	6.26	6.39	6.19	6.09	5.82	5.97	6.17	6.32	6.13	6.03	6.39
11.5	6.14	5.83	6.04	6.13	6.14	6.02	6.29	6.15	6.08	5.75	5.96	6.01	6.24	6.07	5.93	6.31
12.0	6.00	5.72	5.96	6.06	6.03	6.01	6.25	6.09	6.05	5.62	5.93	5.90	6.19	5.93	5.85	6.17
12.5	5.89	5.63	5.87	5.93	5.94	5.89	6.19	6.03	6.01	5.50	5.89	5.81	5.96	5.85	5.82	6.09
13.0	5.80	5.51	5.82	5.85	5.83	5.79	6.09	5.90	5.93	5.47	5.84	5.74	5.97	5.77	5.78	5.88
13.5	5.68	5.45	5.77	5.72	5.66	5.64	5.95	5.76	5.85	5.44	5.73	5.74	5.79	5.62	5.72	5.81
14.0	5.65	5.36	5.72	5.57	5.58	5.52	5.86	5.68	5.75	5.39	5.65		5.76	5.54	5.69	5.74
14.5	5.62	5.33	5.68	5.53	5.51	5.46	5.80	5.56	5.71	5.38	5.60		5.60	5.43	5.67	5.68
15.0	5.62	5.29	5.65	5.49	5.47	5.45	5.66	5.45	5.65	5.38	5.60		5.52	5.36	5.63	5.68
15.5	5.62	5.26	5.65	5.49	5.44	5.45	5.56	5.40	5.65				5.43	5.34		5.68
16.0		5.26		5.49	5.44		5.48	5.40	5.65				5.42	5.33		
16.5							5.48	5.40					5.42	5.33		
17.0							5.48									

Table B-5. Light Transmittance[1] across a 0.25-m path on 28 April 2007

	Light Transmittance (%)															
Depth (m)	**1**	**2**	**3**	**4**	**5**	**6**	**7**	**8**	**9**	**10**	**11**	**12**	**13**	**14**	**15**	**16**
0.5	62.53	60.39		63.02	62.46	62.59	63.08	63.00	62.43	62.93	62.26	60.94	62.15	62.57	62.69	
1.0	62.87	62.96	62.90	62.68	62.57	62.31	62.94	62.98	62.88	62.98	62.49	61.60	62.21	62.71	62.60	62.76
1.5	62.77	62.91	62.78	62.78	62.39	62.45	63.05	62.77	62.72	62.99	62.64	61.94	62.33	62.64	62.65	62.55
2.0	62.92	62.56	62.90	62.73	62.44	62.35	63.10	62.77	63.02	63.20	62.80	62.87	62.13	62.56	62.58	62.70
2.5	62.98	62.75	62.93	62.96	62.45	62.62	63.11	63.05	62.82	63.02	62.92	63.07	63.42	62.93	62.62	62.55
3.0	62.53	62.71	63.03	63.38	62.53	63.09	63.82	63.41	63.05	63.73	63.08	63.54	63.97	63.32	63.07	62.83
3.5	63.08	62.81	63.05	64.32	63.04	64.16	63.86	63.42	63.04	64.88	63.51	64.03	64.20	63.83	64.10	63.38
4.0	63.27	63.85	62.99	65.25	63.69	64.69	63.62	63.40	63.36	65.35	64.75	64.16	64.53	64.81	64.70	63.93
4.5	63.69	64.09	62.43	66.19	64.70	64.83	64.05	63.94	64.15	66.06	65.35	64.18	65.24	65.18	65.33	64.89
5.0	64.42	64.14	61.72	66.23	65.12	65.39	65.30	64.57	65.39	66.21	66.03	65.07	66.00	63.80	65.23	65.07
5.5	64.25	62.86	61.60	65.10	65.70	66.02	66.63	65.34	65.27	65.15	66.17	65.82	66.67	62.74	63.72	65.99
6.0	65.23	61.69	63.17	65.47	65.68	66.99	66.74	66.31	65.34	64.40	66.98	66.28	66.00	63.10	64.26	66.78
6.5	66.46	61.62	64.25	65.63	66.15	67.90	66.91	65.58	65.59	63.81	67.18	66.31	66.37	63.48	64.17	65.89
7.0	67.91	63.58	62.86	65.93	67.55	68.09	67.14	66.26	65.10	60.74	66.48	66.70	66.21	66.52	63.51	64.92
7.5	70.48	65.93	62.48	66.62	67.57	68.00	68.50	66.98	64.62	61.15	64.18	65.73	66.58	68.08	64.81	64.88
8.0	70.45	67.65	62.49	68.05	67.14	69.09	69.09	68.87	63.65	60.53	64.35	66.38	66.84	70.34	67.64	65.69
8.5	71.72	68.06	62.36	67.38	67.98	69.06	70.97	72.23	63.15	61.22	64.37	67.20	68.52	70.94	67.76	66.97
9.0	70.86	69.32	62.30	68.26	67.86	69.85	71.68	71.32	63.49	60.36	63.78	69.64	69.02	70.70	70.06	67.25
9.5	70.29	70.23	63.18	68.96	68.99	70.49	72.00	70.97	63.49	61.93	63.63	70.80	70.61	70.49	70.35	67.56
10.0	70.04	70.46	64.72	68.56	69.55	70.53	71.79	70.89	62.77	61.86	64.13	70.72	70.53	69.93	70.03	67.04
10.5	69.59	70.36	68.75	67.99	69.80	69.70	70.95	70.77	63.12	66.59	63.55	69.98	70.43	69.62	67.94	66.77
11.0	69.41	70.56	70.52	68.95	70.58	70.07	71.12	70.06	65.05	67.59	64.88	70.31	70.19	69.54	64.79	69.03
11.5	69.82	72.02	71.63	68.53	72.91	73.81	71.18	70.54	66.12	63.93	68.09	70.87	70.05	70.44	62.04	71.61
12.0	70.97	73.03	72.32	70.63	73.20	73.33	71.16	70.50	66.82	**58.84**	71.31	73.12	70.45	69.80	62.81	72.62
12.5	72.43	73.33	70.83	73.59	73.80	73.92	71.56	70.71	68.33	**57.40**	70.31	***73.24***	72.19	71.76	61.77	72.89
13.0	73.19	73.50	61.70	73.70	74.63	73.79	71.19	71.19	69.25	56.68	71.01	***69.32***	72.72	73.40	62.44	63.65
13.5	73.20	70.41	57.70	73.19	70.90	66.88	72.02	72.38	70.38	57.25	69.48	***57.86***	73.80	72.66	62.57	**55.62**
14.0	68.54	65.85	58.26	65.70	63.91	59.76	73.83	73.25	71.47	58.10	57.19		74.32	68.23	61.80	54.69
14.5	68.10	63.72	55.65	63.96	60.92	57.07	74.02	73.52	72.06	61.37	**41.93**		71.58	64.85	53.94	55.08
15.0	66.56	57.71	54.74	61.68	59.06	53.05	73.44	70.31	71.87	***59.81***	50.50		64.04	59.14	39.29	49.66
15.5	***55.23***	51.07	56.63	55.01	50.69	41.43	68.39	65.96	64.75				62.00	55.57		36.23
16.0		**35.44**		37.53	46.77		64.81	57.00	51.15				52.79	54.91		
16.5							52.97	46.23					**34.06**	53.31		
17.0							38.32									

[1] Values enclosed in boxes differed significantly from the mean of other transmissivity measurements at the same distance above the seafloor.
The thinner boxes encompass values that were significantly higher than the mean of other measurements at the same distance above the seafloor.

Table B-6. Detrended[1] pH on 28 April 2007

	Hydrogen Ion Concentration (pH)															
Depth (m)	**1**	**2**	**3**	**4**	**5**	**6**	**7**	**8**	**9**	**10**	**11**	**12**	**13**	**14**	**15**	**16**
0.5	7.878	7.871		7.880	7.883	7.888	7.883	7.872	7.882	7.894	7.868	7.893	7.882	7.878	7.878	
1.0	7.878	7.878	7.882	7.882	7.883	7.888	7.883	7.876	7.882	7.889	7.871	7.893	7.885	7.878	7.879	7.887
1.5	7.882	7.879	7.882	7.886	7.885	7.888	7.886	7.880	7.887	7.893	7.875	7.893	7.891	7.883	7.884	7.885
2.0	7.885	7.884	7.885	7.886	7.887	7.888	7.887	7.889	7.886	7.893	7.885	7.893	7.893	7.886	7.888	7.891
2.5	7.888	7.889	7.886	7.886	7.887	7.891	7.892	7.890	7.886	7.886	7.888	7.889	7.899	7.888	7.892	7.895
3.0	7.894	7.893	7.886	7.887	7.887	7.893	7.892	7.892	7.886	7.881	7.889	7.886	7.894	7.890	7.892	7.897
3.5	7.893	7.894	7.886	7.881	7.887	7.892	7.893	7.888	7.886	7.878	7.889	7.883	7.894	7.884	7.889	7.895
4.0	7.893	7.887	7.885	7.864	7.888	7.877	7.893	7.886	7.892	7.870	7.881	7.872	7.883	7.872	7.885	7.880
4.5	7.888	7.877	7.884	7.842	7.881	7.863	7.882	7.893	7.890	7.846	7.869	7.860	7.877	7.859	7.859	7.871
5.0	7.876	7.869	7.860	7.813	7.874	7.841	7.872	7.877	7.879	7.827	7.860	7.841	7.866	7.842	7.844	7.868
5.5	7.869	7.845	7.824	7.796	7.865	7.827	7.851	7.860	7.873	7.818	7.846	7.828	7.832	7.820	7.834	7.840
6.0	7.843	7.823	7.787	7.767	7.832	7.813	7.829	7.835	7.851	7.797	7.829	7.824	7.821	7.777	7.791	7.824
6.5	7.821	7.813	7.757	7.744	7.810	7.794	7.814	7.828	7.846	7.784	7.821	7.811	7.800	7.773	7.764	7.806
7.0	7.792	7.772	7.750	7.694	7.794	7.779	7.805	7.803	7.834	7.750	7.800	7.795	7.781	7.750	7.749	7.778
7.5	7.781	7.753	7.743	7.699	7.777	7.755	7.777	7.790	7.817	7.749	7.786	7.789	7.764	7.736	7.737	7.751
8.0	7.773	7.738	7.724	7.698	7.755	7.743	7.764	7.751	7.802	7.732	7.776	7.776	7.746	7.730	7.713	7.726
8.5	7.760	7.730	7.707	7.693	7.738	7.738	7.748	7.735	7.794	7.721	7.764	7.773	7.738	7.724	7.721	7.720
9.0	7.753	7.728	7.708	7.690	7.733	7.732	7.742	7.731	7.762	7.712	7.759	7.767	7.732	7.720	7.718	7.720
9.5	7.742	7.717	7.702	7.687	7.727	7.724	7.736	7.717	7.760	7.709	7.756	7.760	7.729	7.711	7.716	7.715
10.0	7.729	7.707	7.698	7.684	7.721	7.720	7.730	7.710	7.746	7.703	7.757	7.754	7.727	7.706	7.712	7.712
10.5	7.725	7.701	7.697	7.682	7.718	7.718	7.729	7.704	7.749	7.697	7.760	7.751	7.726	7.702	7.711	7.705
11.0	7.714	7.696	7.697	7.682	7.716	7.716	7.726	7.702	7.741	7.703	7.758	7.746	7.723	7.697	7.705	7.697
11.5	7.709	7.691	7.695	7.677	7.707	7.702	7.717	7.699	7.735	7.708	7.754	7.740	7.722	7.693	7.697	7.694
12.0	7.702	7.685	7.691	7.678	7.700	7.704	7.717	7.696	7.730	7.708	7.750	7.734	7.723	7.689	7.690	7.686
12.5	7.698	7.679	7.687	7.670	7.698	7.695	7.717	7.693	7.730	7.704	7.744	7.730	7.716	7.684	7.689	7.684
13.0	7.693	7.672	7.683	7.666	7.694	7.692	7.715	7.689	7.730	7.699	7.741	7.727	7.715	7.677	7.683	7.676
13.5	7.687	7.665	7.676	7.661	7.689	7.684	7.713	7.684	7.732	7.692	7.741	7.720	7.708	7.672	7.676	7.672
14.0	7.684	7.662	7.672	7.657	7.680	7.674	7.703	7.682	7.737	7.694	7.739		7.703	7.670	7.675	7.668
14.5	7.678	7.658	7.667	7.652	7.674	7.669	7.694	7.674	7.736	7.694	7.733		7.700	7.663	7.675	7.662
15.0	7.675	7.655	7.664	7.648	7.666	7.664	7.689	7.671	7.735	7.699	7.731		7.693	7.656	7.660	7.661
15.5	7.664	7.649	7.664	7.641	7.663	7.661	7.685	7.661	7.729				7.685	7.654		7.652
16.0		7.646		7.640	7.658		7.676	7.652	7.727				7.683	7.651		
16.5							7.670	7.654					7.678	7.651		
17.0							7.670									

[1] Measured pH levels were corrected for temporal drift to account for ongoing equilibration of the pH sensor.

Table B-7. Uncorrected pH on 28 April 2007

	Alkalinity (pH)															
Depth (m)	**1**	**2**	**3**	**4**	**5**	**6**	**7**	**8**	**9**	**10**	**11**	**12**	**13**	**14**	**15**	**16**
0.5	7.878	7.865		7.867	7.869	7.873	7.864	7.841	7.803	7.780	7.740	7.718	7.867	7.878	7.878	
1.0	7.878	7.872	7.869	7.869	7.869	7.873	7.864	7.845	7.803	7.775	7.743	7.718	7.870	7.878	7.879	7.887
1.5	7.882	7.873	7.869	7.873	7.871	7.873	7.867	7.849	7.808	7.779	7.747	7.718	7.876	7.883	7.884	7.885
2.0	7.885	7.878	7.872	7.873	7.873	7.873	7.868	7.858	7.807	7.779	7.757	7.718	7.878	7.886	7.888	7.891
2.5	7.888	7.883	7.873	7.873	7.873	7.876	7.873	7.859	7.807	7.772	7.760	7.714	7.884	7.888	7.892	7.895
3.0	7.894	7.887	7.873	7.874	7.873	7.878	7.873	7.861	7.807	7.767	7.761	7.711	7.879	7.890	7.892	7.897
3.5	7.893	7.888	7.873	7.868	7.873	7.877	7.874	7.857	7.807	7.764	7.761	7.708	7.879	7.884	7.889	7.895
4.0	7.893	7.881	7.872	7.851	7.874	7.862	7.874	7.855	7.813	7.756	7.753	7.697	7.868	7.872	7.885	7.880
4.5	7.888	7.871	7.871	7.829	7.867	7.848	7.863	7.862	7.811	7.732	7.741	7.685	7.862	7.859	7.859	7.871
5.0	7.876	7.863	7.847	7.800	7.860	7.826	7.853	7.846	7.800	7.713	7.732	7.666	7.851	7.842	7.844	7.868
5.5	7.869	7.839	7.811	7.783	7.851	7.812	7.832	7.829	7.794	7.704	7.718	7.653	7.817	7.820	7.834	7.840
6.0	7.843	7.817	7.774	7.754	7.818	7.798	7.810	7.804	7.772	7.683	7.701	7.649	7.806	7.777	7.791	7.824
6.5	7.821	7.807	7.744	7.731	7.796	7.779	7.795	7.797	7.767	7.670	7.693	7.636	7.785	7.773	7.764	7.806
7.0	7.792	7.766	7.737	7.681	7.780	7.764	7.786	7.772	7.755	7.636	7.672	7.620	7.766	7.750	7.749	7.778
7.5	7.781	7.747	7.730	7.686	7.763	7.740	7.758	7.759	7.738	7.635	7.658	7.614	7.749	7.736	7.737	7.751
8.0	7.773	7.732	7.711	7.685	7.741	7.728	7.745	7.720	7.723	7.618	7.648	7.601	7.731	7.730	7.713	7.726
8.5	7.760	7.724	7.694	7.680	7.724	7.723	7.729	7.704	7.715	7.607	7.636	7.598	7.723	7.724	7.721	7.720
9.0	7.753	7.722	7.695	7.677	7.719	7.717	7.723	7.700	7.683	7.598	7.631	7.592	7.717	7.720	7.718	7.720
9.5	7.742	7.711	7.689	7.674	7.713	7.709	7.717	7.686	7.681	7.595	7.628	7.585	7.714	7.711	7.716	7.715
10.0	7.729	7.701	7.685	7.671	7.707	7.705	7.711	7.679	7.667	7.589	7.629	7.579	7.712	7.706	7.712	7.712
10.5	7.725	7.695	7.684	7.669	7.704	7.703	7.710	7.673	7.670	7.583	7.632	7.576	7.711	7.702	7.711	7.705
11.0	7.714	7.690	7.684	7.669	7.702	7.701	7.707	7.671	7.662	7.589	7.630	7.571	7.708	7.697	7.705	7.697
11.5	7.709	7.685	7.682	7.664	7.693	7.687	7.698	7.668	7.656	7.594	7.626	7.565	7.707	7.693	7.697	7.694
12.0	7.702	7.679	7.678	7.665	7.686	7.689	7.698	7.665	7.651	7.594	7.622	7.559	7.708	7.689	7.690	7.686
12.5	7.698	7.673	7.674	7.657	7.684	7.680	7.698	7.662	7.651	7.590	7.616	7.555	7.701	7.684	7.689	7.684
13.0	7.693	7.666	7.670	7.653	7.680	7.677	7.696	7.658	7.651	7.585	7.613	7.552	7.700	7.677	7.683	7.676
13.5	7.687	7.659	7.663	7.648	7.675	7.669	7.694	7.653	7.653	7.578	7.613	7.545	7.693	7.672	7.676	7.672
14.0	7.684	7.656	7.659	7.644	7.666	7.659	7.684	7.651	7.658	7.580	7.611		7.688	7.670	7.675	7.668
14.5	7.678	7.652	7.654	7.639	7.660	7.654	7.675	7.643	7.657	7.580	7.605		7.685	7.663	7.675	7.662
15.0	7.675	7.649	7.651	7.635	7.652	7.649	7.670	7.640	7.656	7.585	7.603		7.678	7.656	7.660	7.661
15.5	7.664	7.643	7.651	7.628	7.649	7.646	7.666	7.630	7.650				7.670	7.654		7.652
16.0		7.640		7.627	7.644		7.657	7.621	7.648				7.668	7.651		
16.5							7.651	7.623					7.663	7.651		
17.0							7.651									

Table B-8. Ancillary Observations on 28 April 2007 during the Receiving-Water Survey

	Location		Diffuser Distance	Time	Air Temperature	Cloud Cover	Wind Avg	Wind Max	Wind Dir (from)	Swell Ht/Dir	Secchi Depth
Station	Latitude	Longitude	(m)	(PDT)	(°C)	(%)	(kt)	(kt)	(°T)	(ft/°T)	(m)
1	35° 23.256' N	120° 52.501' W	106.5	07:47:04	12.6	10	2.0	3.1	WNW	3-4/W	3.0
2	35° 23.236' N	120° 52.511' W	69.5	07:43:57	13.8	10	1.7	3.1	WNW	3-4/W	3.0
3	35° 23.212' N	120° 52.501' W	24.9	07:41:11	13.1	10	1.1	2.4	WNW	3-4/W	3.0
4	35° 23.192' N	120° 52.499' W	16.0	07:36:12	14.5	10	1.2	2.2	S	3-4/W	3.0
5	35° 23.171' N	120° 52.500' W	52.2	07:32:57	13.5	10	1.3	2.5	S	3-4/W	3.0
6	35° 23.156' N	120° 52.496' W	81.8	07:30:29	13.8	10	1.3	3.3	S	3-4/W	3.0
7	35° 23.206' N	120° 52.565' W	92.2	07:20:05	14.9	10	1.9	4.1	SW	3-4/W	3.0
8	35° 23.203' N	120° 52.546' W	63.7	07:16:42	15.9	10	2.1	4.5	SW	3-4/W	3.0
9	35° 23.199' N	120° 52.515' W	16.5	07:13:25	15.7	10	1.8	3.9	SW	3-4/W	3.0
10	35° 23.207' N	120° 52.486' W	30.2	07:10:17	14.2	10	1.8	3.9	SW	3-4/W	3.0
11	35° 23.197' N	120° 52.458' W	70.5	07:05:54	13.1	10	2.8	6.0	SW	3-4/W	3.0
12	35° 23.205' N	120° 52.434' W	107.4	07:02:13	15.9	10	1.4	3.0	SW	3-4/W	3.0
13	35° 23.176' N	120° 52.523' W	51.5	07:24:11	14.9	10	1.9	4.1	S	3-4/W	3.0
14	35° 23.226' N	120° 52.528' W	62.1	07:51:26	12.9	10	1.4	2.5	WNW	3-4/W	3.0
15	35° 23.225' N	120° 52.468' W	72.9	07:56:20	14.3	10	1.3	3.9	WNW	3-4/W	3.0
16	35° 23.176' N	120° 52.471' W	66.1	08:00:40	13.8	10	1.2	3.3	WNW	3-4/W	3.0

There was no visual expression of the effluent plume at the sea surface. Neither odors nor debris of sewage origin were observed at any time during the survey. Winds were light and variable and occasional breezes from canyons onshore caused air temperature to fluctuate.

Tidal Conditions (Pacific Daylight Time)
Low Tide: 03:01 0.84 ft
High Tide: 08:53 3.92 ft
Low Tide: 14:50 0.62 ft
High Tide: 21:09 4.72 ft